RESEARCH ACTIVITIES in

Automatic Controls — Antennas — Echo Area Studies
Microwave Circuits — Astronautics — EM Field Theory
Theory Investigations — Plasmas — Systems Analysis
Wave Propagation — Submillimeter Applications

X66 35161	
(ACCESSION NUMBER)	(THRU)
44	2A
(PAGES)	(CODE)
CR 68642	07
(NASA CR OR TMX OR AD NUMBER)	(CATEGORY)

FACILITY FORM 602

Power Spectral Analysis of Echo ... Reflected Signals

Report to ...

Grant Number NsG-...

... 31 December 196...

Prepared for
National Aeronautics and Space Administration
Goddard Space Flight Center
Greenbelt, Maryland

NOTICES

When Government drawings, specifications, or other data are used for any purpose other than in connection with a definitely related Government procurement operation, the United States Government thereby incurs no responsibility nor any obligation whatsoever, and the fact that the Government may have formulated, furnished, or in any way supplied the said drawings, specifications, or other data, is not to be regarded by implication or otherwise as in any manner licensing the holder or any other person or corporation, or conveying any rights or permission to manufacture, use, or sell any patented invention that may in any way be related thereto.

The Government has the right to reproduce, use, and distribute this report for governmental purposes in accordance with the contract under which the report was produced. To protect the proprietary interests of the contractor and to avoid impairment of its obligations to the Government, this report may not be released for non-governmental use such as might constitute general publication without the express prior consent of The Ohio State University Research Foundation.

Qualified requesters may obtain copies of this report from the Defense Documentation Center, Cameron Station, Alexandria, Virginia. Department of Defense contractors must be established for DDC services, or have their "need-to-know" certified by the cognizant military agency of their project or contract.

REPORT

by

THE OHIO STATE UNIVERSITY RESEARCH FOUNDATION
COLUMBUS, OHIO 43212

Sponsor	National Aeronautics & Space Administration Goddard Space Flight Center Glen Dale Road Greenbelt, Maryland 20771
Grant Number	NAS5-9507
Investigation of	Tracking, Receiving, Recording and Analysis of Data from Echo Satellite
Subject of Report	Power Spectral Density of Echo II Reflected Signals
Submitted by	Stephen L. Zolnay Antenna Laboratory Department of Electrical Engineering
Date	31 December 1964

TABLE OF CONTENTS

		Page
I.	INTRODUCTION	1
II.	POWER SPECTRAL DENSITY CURVES OF PASSIVE SATELLITE-REFLECTED SIGNALS OBTAINED BY THE ANALOG METHOD	3
III.	POWER SPECTRAL DENSITY CURVES OF PASSIVE SATELLITE REFLECTED SIGNALS OBTAINED BY THE DIGITAL METHOD	5
IV.	SUMMARY	7
V.	ACKNOWLEDGEMENTS	17
REFERENCES		18
VI.	APPENDIX	21
	A. Data Collection, Reduction, and Analysis	21
	B. Data Collection	21
	1. System Description	21
	2. Format for collected data	27
	C. Data Reduction and Analysis	30
	1. Signal strength	30
	2. Echo area	33
	3. Autocorrelation, probability density, and power spectral density functions	33
	a. Digital method	33
	b. Analog method	38
	4. Depolarization effects	40

POWER SPECTRAL DENSITY OF ECHO II REFLECTED SIGNALS

I. INTRODUCTION

This report deals with the power spectra of passive satellite-reflected signals. The receiving site is The Ohio State University Satellite Communications Center; the transmitting site is the Collins Space Communications Facility, Dallas, Texas. The passive satellites utilized were Echo I and Echo II; the signal was cw at 2260 Mc/sec. The main objective was to obtain the power spectra of signals reflected by Echo II; the power spectra of Echo I reflected signals are included for comparison. The purpose of this report is to present experimental data, to analyze reduced experimental data, and to describe the methods by which the data were collected and processed.

A sample of the experimental data is shown in Fig. 1. The signal originated from Dallas as cw at 2260 Mc/sec and was reflected by Echo I during revolution 2626. The amplitude of the transmitted signal was known within one db and it was constant within less than one db. Tracking inaccuracies, gain instabilities, and other effects could have contributed, at the most, two to three db to the amplitude variations. However, the variations in the amplitude of the received signal exceeded, by at least one order of magnitude, the variations that could be ascribed to equipment instabilities. The received signal was down-converted to baseband and amplitude de-modulated. The output voltage of the detector (shown in Fig. 1) is proportional to the amplitude modulation present on the cw signal, and appears to be a randomly varying quantity. To obtain information about the frequencies present in the signal the power spectral density of the detector output was obtained; the PSD curves were obtaine by the analog technique. Description of the analog equipment is given in the Appendix; the passband characteristic of this equipment and the band width of the filter in it, as well as the effect of these on the PSD curves, not considered here. The power spectrum of a signal can also be obtaine by Fourier transformation from its autocorrelation function. This proced has been adapted by R.T. Compton[2] to the particular problem of Echo-reflected signals and the autocorrelation functions thereof; it is also included in the Appendix. There are numerous autocorrelation functions available which were obtained by digital technique from sampled data. The PSD curves obtained from these ACFs are also included in this repo

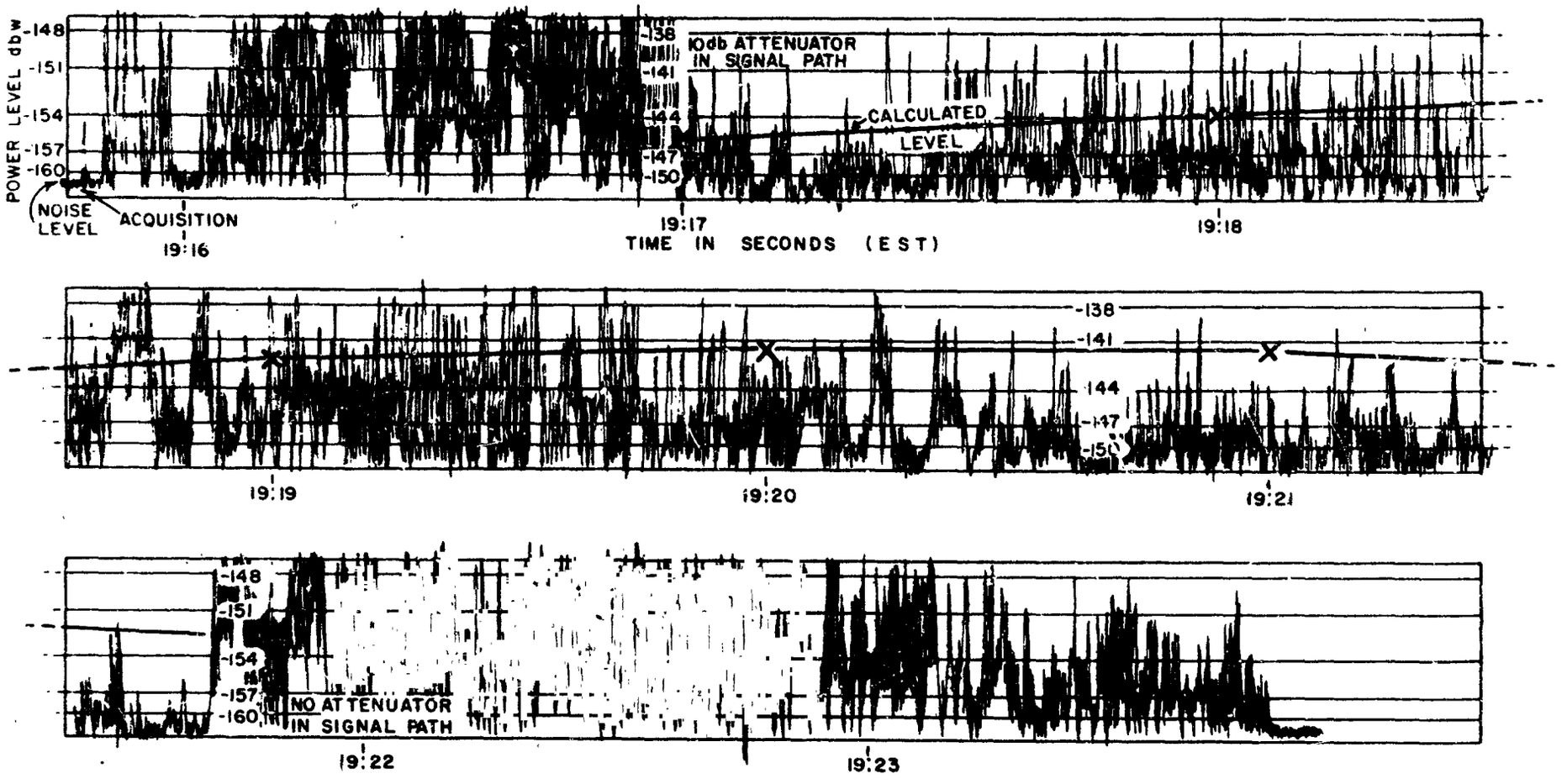

Fig. 1. Sample of received cw signal--Echo II revolution 2626.

Detailed description of the receiving system has been published by Eberle[3]; an accurate description of the transmitting site is also available.[4]

II. POWER SPECTRAL DENSITY CURVES OF PASSIVE SATELLITE-REFLECTED SIGNALS OBTAINED BY THE ANALOG METHOD

The power spectral density curves of passive satellite-reflected signals obtained by the analog method are shown in Figs. 2-8. These were obtained from cw signals reflected by Echo II during revolutions 2626, 2653, 2816, 3040, and 3483, and by Echo I during revolutions 18,166 and 18,966. The data from which these PSD curves were made were representative of all cw data collected on Echo II revolutions 2000-3500, and Echo I data were selected from the same period during which the above Echo II revolutions occurred.

These figures show that most of the energy is between zero and about twelve cps. Higher frequency components, if present in the original signal, contribute negligibly to the frequency spectrum. PSD analysis on other Echo data was carried out to a maximum of 250 cps verifying the above statement experimentally.[1] Since the very early revolutions of Echo II it has been observed that a periodic fading occurred on the signal originating from the telemetry transmitters. From a knowledge of the location of these transmitters and from the fadings observed it was concluded that Echo II was rotating and a period of 100 seconds per revolution was claimed. Were this indeed true, then for a configuration such that the axis of rotation of the balloon and the line of sight of the antenna were perpendicular to each other, a maximum spread in the carrier frequency due to doppler would result. The maximum shift in the above situation for monostatic operation and carrier frequency at 2260 Mc/sec would originate from the limbs of the balloon; for Echo II it would be about 20 cps. Thus, the maximum frequencies present in the spectra should be about 20 cps. All figures of PSD for Echo II, and also for Echo I, show spectral broadening which, however, does not extend to 20 cps. In fact, at 12 cps the amplitude of the spectral curves is 10% or less of maximum amplitude.

Two spectral curves are shown in Fig. 2 for data obtained on Echo II revolution 2626. The data from which Fig. 2a was obtained indicated a high signal-to-noise ratio, greater than +10 dbs, and the data for Fig. 2b indicated low signal-to-noise ratio, less than +10 dbs. There is no appreciable difference between the two curves, indicating a reasonable accuracy in the procedure of obtaining the PSD curves. The accuracy of these curves was

increased by linearizing the data before they were applied to the power spectral density analyzer. In a complex system, such as the one used for receiving the satellite-reflected signals, some nonlinearities are usually present. It was found to be easier to compensate for equipment nonlinearities than to eliminate them. Description of the analog compensating equipment and illustration of its use were given by Groves.[5]

The possibility that Echo II is rotating has been pointed out in preceding discussion. A phenomenon that could readily be explained with a postulated rotation of the satellite has been observed repeatedly. Figure 1 shows a sample of the data analogous to the received signal strength. It can be seen that the fluctuations are quite rapid, i.e., upwards to 10 cps. On occasion it has been observed that the amplitude scintillations slow down considerably. Counting the maxima and minima, it has been established that the condition for which there were one, or less, maximum and minimum per second lasted about two minutes. If one accepts an explanation in terms of doppler-shifted frequencies and interactions between them for the origin of the rapid fluctuations, such as the ones shown in Fig. 1, then the condition for which the rate of fluctuations is very slow calls for relatively no doppler shift. Such would be the case if the axis of rotation of the satellite and the line of sight to the antenna were essentially coincident. Then all the visible portions of the satellite would appear to move with the same velocity, hence the doppler shift would be minimum. Figure 3a was produced from data obtained during revolution 2653 when the scintillation rate was normal; Fig. 3b was produced from that portion of the pass during which this rate was at a minimum. The spectral curve in Fig. 3b is much narrower, as could be expected, indicating that most of the energy is close to dc.

Three other Echo II passes have been analyzed. The PSD curves from these three passes are shown in Figs. 4-6. These curves are not appreciably different from the preceding ones; they all show very low amplitudes beyond 10 cps and indicate that most of the energy is around dc. The accurate measurement of the spectrum very close (less than half a cycle) to dc is not possible with the analyzing equipment. The less-than-unity amplitudes near dc shown in Figs. 2-8 are caused by the passband characteristics of the analyzing equipment.

The PSD curves of the two Echo I passes selected for comparison with those obtained from Echo II-reflected signals are given in Figs. 7 and 8. The shape of these spectral curves is very similar to those of Echo II curves. They also indicate maximum energy near dc and show that the amplitude by 12 cps is about 10% of the maximum amplitude. They are apparently narrower, however, than the Echo II curves. Since no rotation has ever been claimed for Echo I, the similarity of the PSD curves obtained from the two satellites raises the possibility

of existence of some mechanism which causes spectral broadening and which is common to both satellites. Such a mechanism could be ionospheric and/or atmospheric irregularities. It has been observed and reported earlier[1] that a small but perceptible change in the spectrum occurred as the position of the satellite changed during a pass. This observation, however, requires more extensive documentation because the frequency of operation is such that ionospheric effects should no longer be significant and atmospheric effects should still be negligibly small. Anotner possibility, of course, is that much of the spectral broadening originates right at the transmitter. To produce a very clear signal at a frequency of 2260 Mc/sec an accuracy of one part in 10^9 is required; it is doubtful that such accuracy was maintained during transmission. The best available estimate from the transmitter side* puts the accuracy of the transmitted frequency at a few parts in 10^8. Thus, until spectral density curves of the transmitted signal become available, it is difficult to arrive at conclusions about the broadness of the spectra or the mechanism(s) causing spectral broadening. However, it can be stated that the spectra of Echo I- and Echo II-reflected signals are remarkably similar.

In conclusion, it can be said that the power spectral density curves of passive satellite-reflected signals obtained by analog techniques from linearized data indicate the following:

(1) maximum energy content is near dc,

(2) the amplitude at 12 cps is 10% or less of maximum amplitude, and

(3) there is a remarkable similarity between Echo I and Echo II curves.

III. POWER SPECTRAL DENSITY CURVES OF PASSIVE SATELLITE REFLECTED SIGNALS OBTAINED BY THE DIGITAL METHOD

The power spectral density curves of passive satellite-reflected signals obtained from the autocorrelation function by Fourier Transform technique are shown in Figs. 10-16. A small digital computer was utilized to obtain these data. The curves were prepared from data obtained during the same revolution as the ones used to obtain Figs. 2-8. The

---

*Private communication with Collins personnel.

maximum difference in time between the intervals used for the analog and digital curves is about two minutes; whenever possible the exact same interval of data for both types of curves was used. The frequency resolution inherent in the autocorrelation functions is much better than in the PSD curves obtained by the analog method. The resolution of the filter in the analog analyzing equipment was measured and found to be about 3 cps. The autocorrelation function was obtained by digitizing the data at the rate of 50 samples per second and using a sample length of 30 seconds. Had the sample length been infinite and had there been a periodic component at a frequency ω_o present in the original data, then the autocorrelation function would have also contained this periodic component. The finite sample length and the sampling rate introduces an error in the ACF. The magnitude of this error can readily be estimated; it is on the order of $1/\omega_o T$, where T is the sample length. It is seen that the maximum error occurs for the slowest frequency. Solodovnikov[6] shows that for a 2% accuracy in the autocorrelation function the sample length must be equal to at least 10 T_o, where $T_o = 1/f_o$, and the maximum time delay must be less than $2T_o$. Based on these figures, it may be stated that the 30-second sample length permitted a 2% accuracy to frequencies of 1/3 cps. The maximum time delay was always equal to $1T_o$. This is not necessarily the accuracy of the PSD curves produced for the ACFs, but it is safe to assume that these PSD curves are at least several times more accurate than the ones produced with a filter whose half-power bandwidth was about 3 cps.

As it could have been expected, the better resolution inherent in the digital method, as compared with the analog method, has yielded more and finer detail in the power spectral density curves. In all of Figs. 10-16 the maximum energy content is shown to be at, or very near, zero frequency. This effect can be observed much better in these figures than in Figs. 2-8. A monochromatic signal reflected by a perfect sphere would yield a spectrum of a single impulse at f = 0. In the present case ideal conditions such as monochromatic signal and perfect surface for Echoes cannot be assumed. Both the roughness and the relative motion of the satellites contribute to the spectral broadening. The large amplitudes close to dc, however, indicate that these PSD curves could be regarded as composed of two parts: a narrow portion of large amplitude at dc and a broad portion of relatively low amplitude, decreasing with frequency and extending to 8 cps or more. The narrow spectrum at dc would be associated with the specular return from the flare spot on the reflector, and the broad portion of the spectrum would be associated with the diffuse return. Figure 9 illustrates this idea. It can be stated that both Echoes have spectra indicating large specular returns from which it can be implied that these satellites at 2260 Mc/sec appear to be very

good reflectors. From the spectral broadening observed in all spectra it can be implied that the surface of Echoes is rough. It should be pointed out again that the spectra of Echo I and of Echo II are remarkably similar, even to the extent of observed maximum spectral broadening.

The power spectral density curves of Echo satellite-reflected signals obtained by digital techniques, with improved frequency resolution from linearized data indicate the following:

1. Maximum energy content is between dc and one cps,

2. The energy content by 8 cps and beyond that frequency is negligibly small, and

3. Echo I and Echo II are very similar.

IV. SUMMARY

This report deals with the power spectra of Echo-reflected signals. Echo II data are emphasized; some Echo I data are also included. The signal was CW at 2260 Mc/sec, and the data were selected from Echo II revolutions 2000-3500. Data collection, reduction, and analysis are considered in the Appendix. The power spectra were obtained by analog and digital techniques. The frequency resolution in the analog PSDs was about 3 cps; much improved resolution was obtained by the digital technique. On the basis of both these analyses it is concluded the maximum energy is between dc and one cps, indicating large specular return from these satellites. From this fact it can be implied that they are very good reflectors at this frequency. It is also concluded that broadening is present in all spectra which extend to about 8 cps; beyond 8 cps, however, the amplitude of the spectral curves is negligibly small indicating probable rough surfaces of Echoes, and indicating that the amplitude scintillations faster than 8 cps are negligible relative to the amplitude scintillations that are slower than 8 cps. The spectral curves of Echo I and of Echo II were found to be remarkably similar.

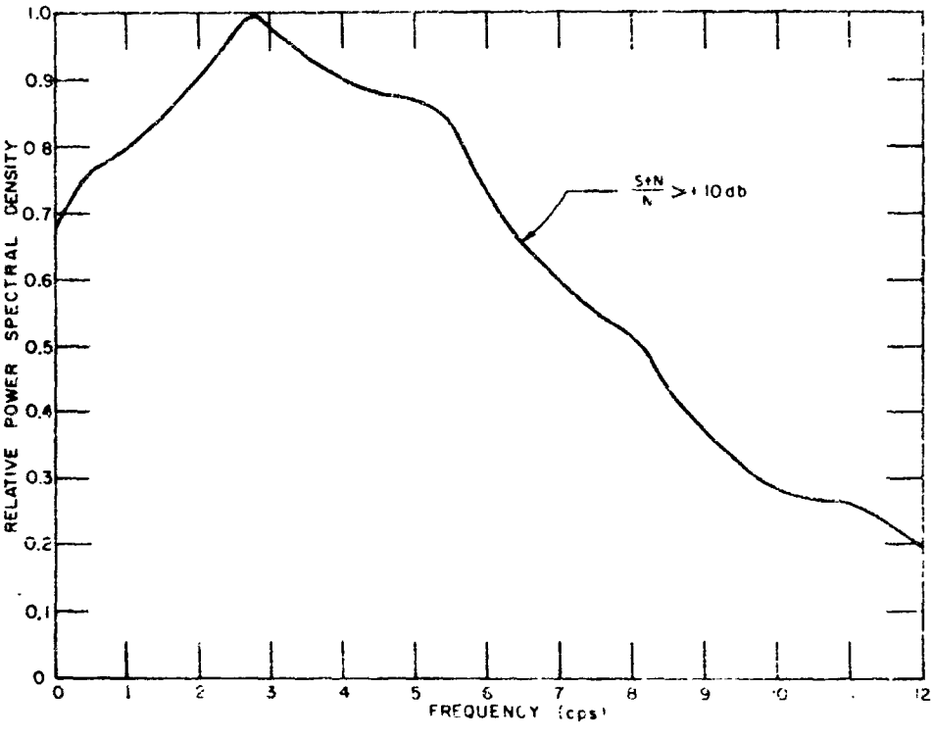

(a) Signal-to-noise ratio above +10 db

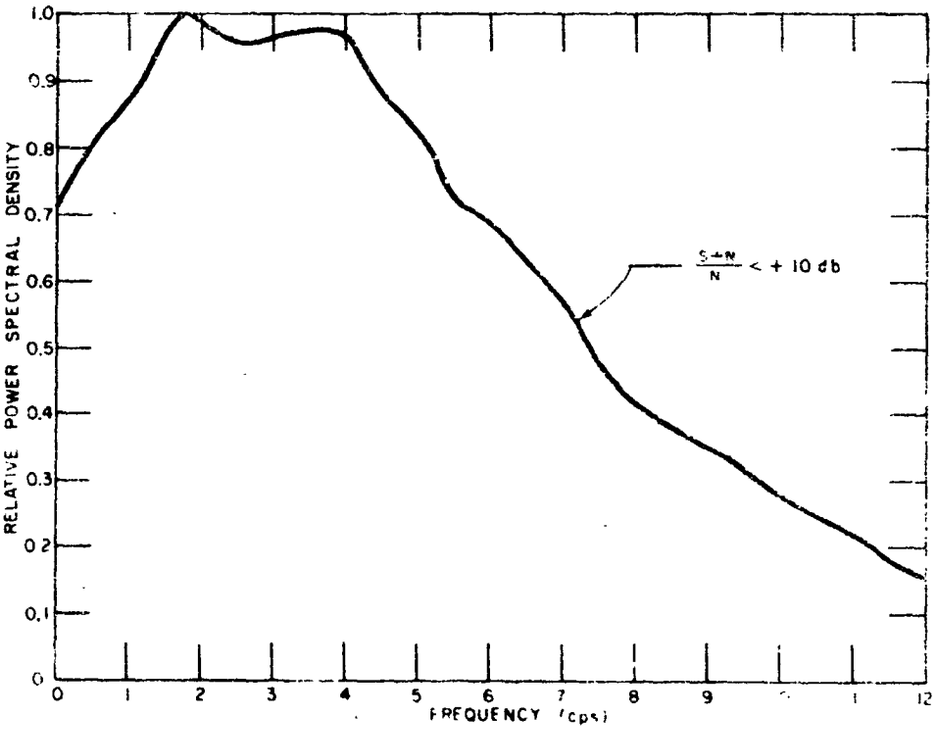

(b) Signal-to-noise ratio below + 10 db

Fig. 2. Analog PSD curve of a cw signal reflected by Echo II during revolution 2626.

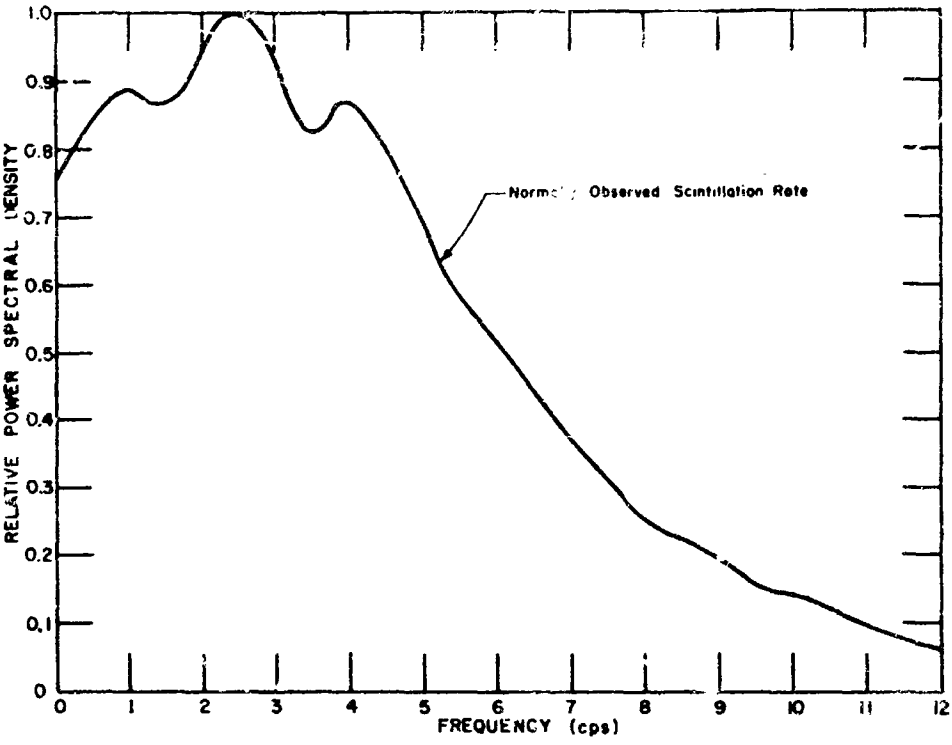

(a) Normally observed scintillation rate

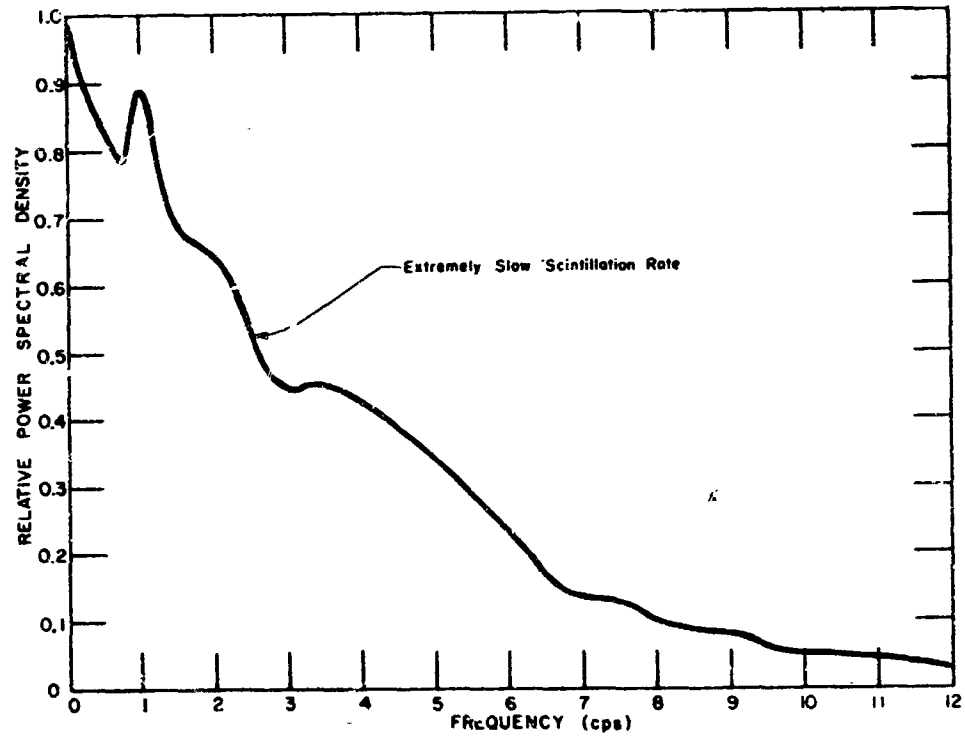

(b) Very slow scintillation rate (one or less maximum and minimum per second)

Fig. 3. Analog PSD curve of a cw signal reflected by Echo II during revolution 2653

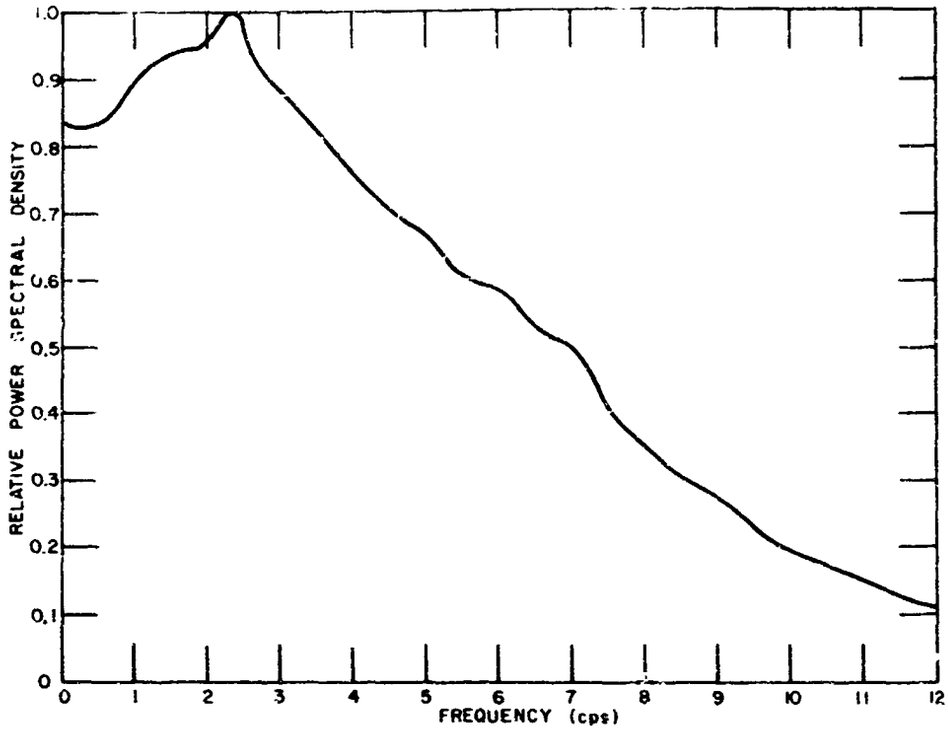

Fig. 4. Analog PSD curve of a cw signal reflected by Echo II during revolution 2816.

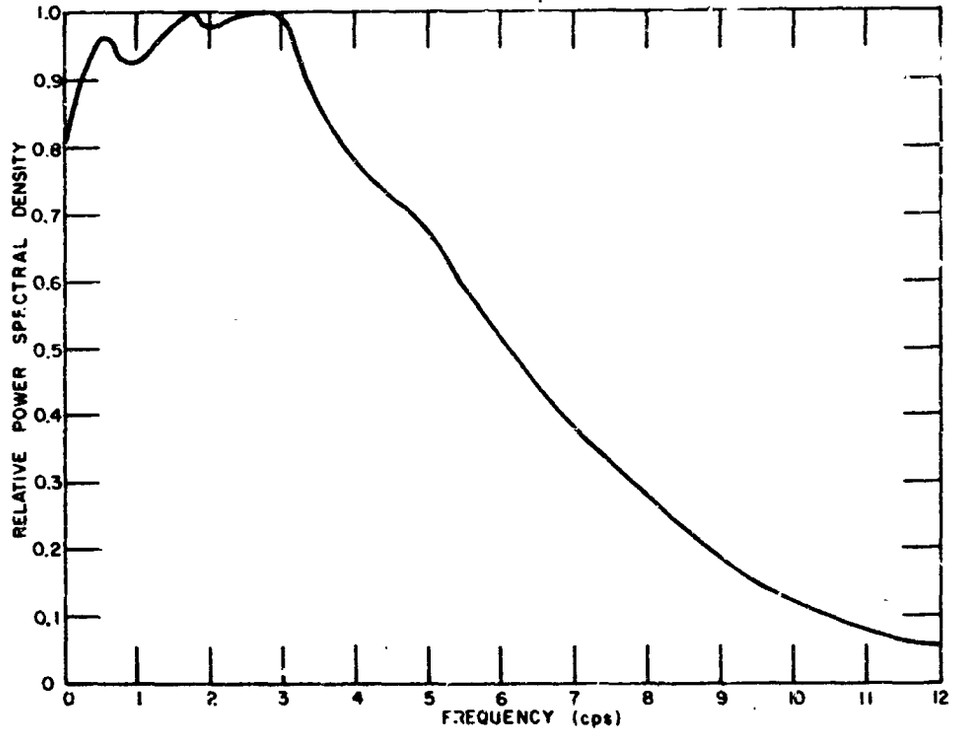

Fig. 5. Analog PSD curve of a cw signal reflected by Echo II during revolution 3040.

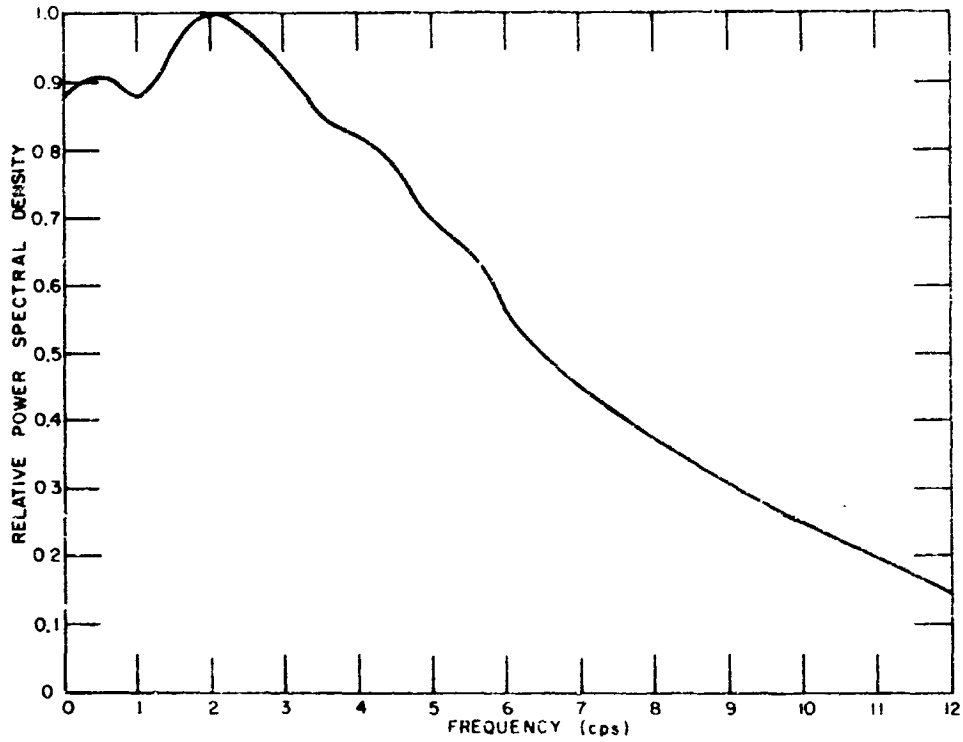

Fig. 6. Analog PSD curve of a cw signal reflected by Echo II during revolution 3483.

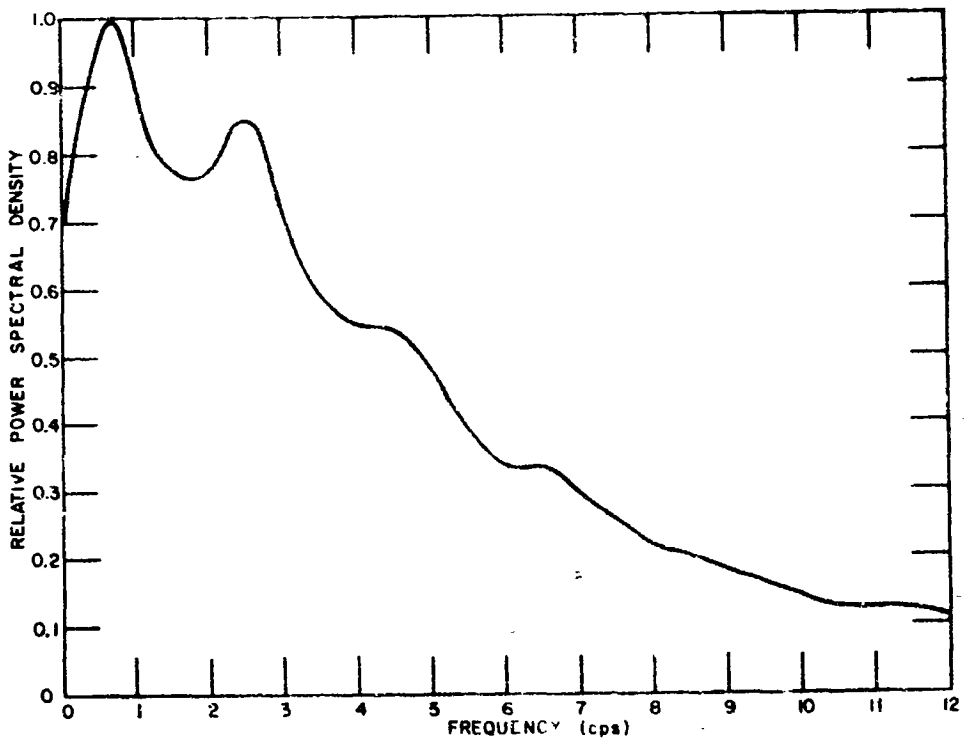

Fig. 7. Analog PSD curve of a cw signal reflected by Echo I during revolution 18, 166.

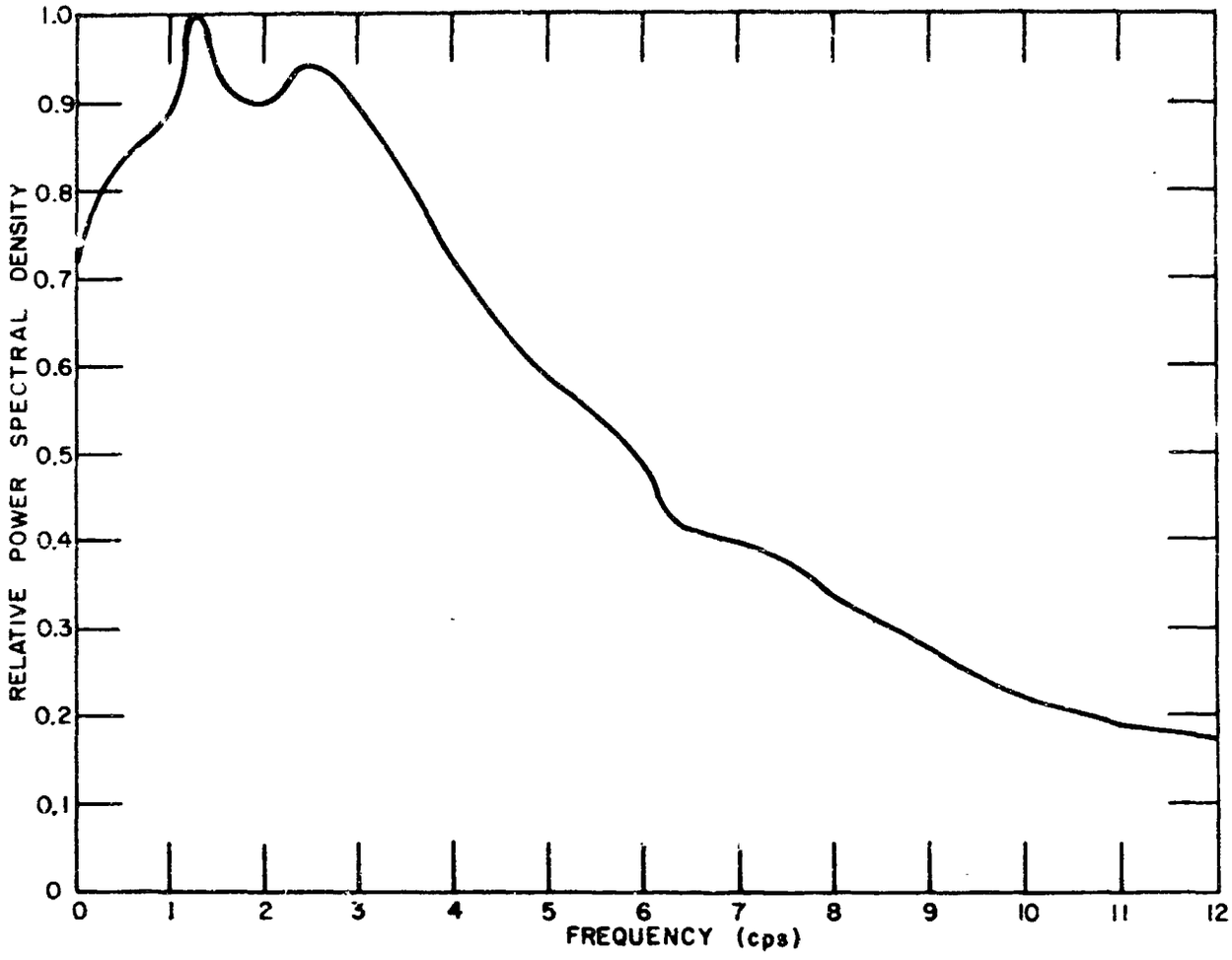

Fig. 8. Analog PSD curve of a cw signal reflected by Echo I during revolution 18,966.

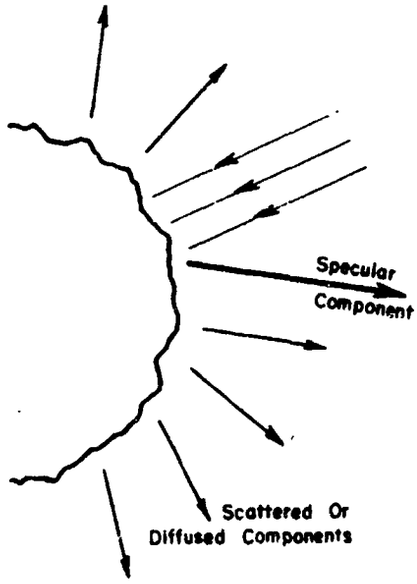

Fig. 9. Specular and diffuse components of a signal reflected by a rough surface.

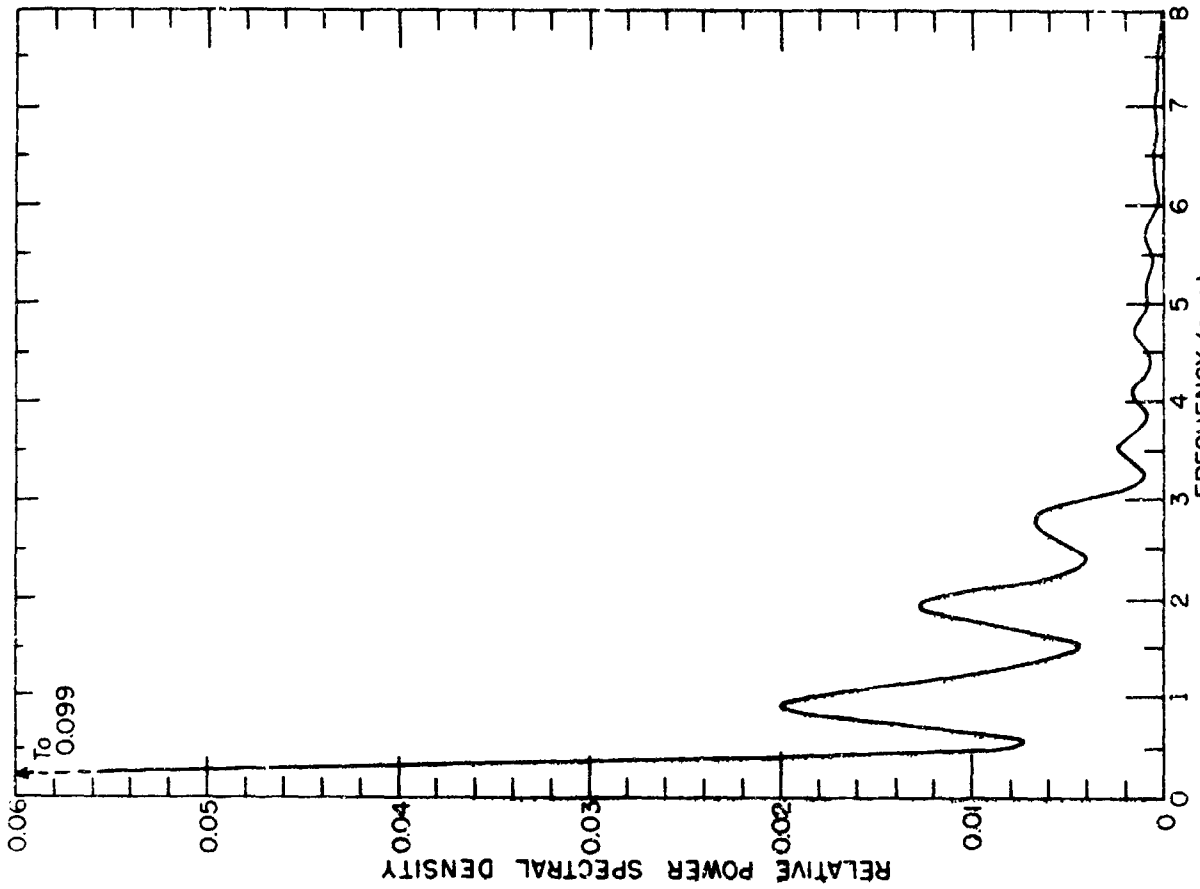

Fig. 11. Digital PSD curve of a cw signal reflected by Echo II during revolution 2653.

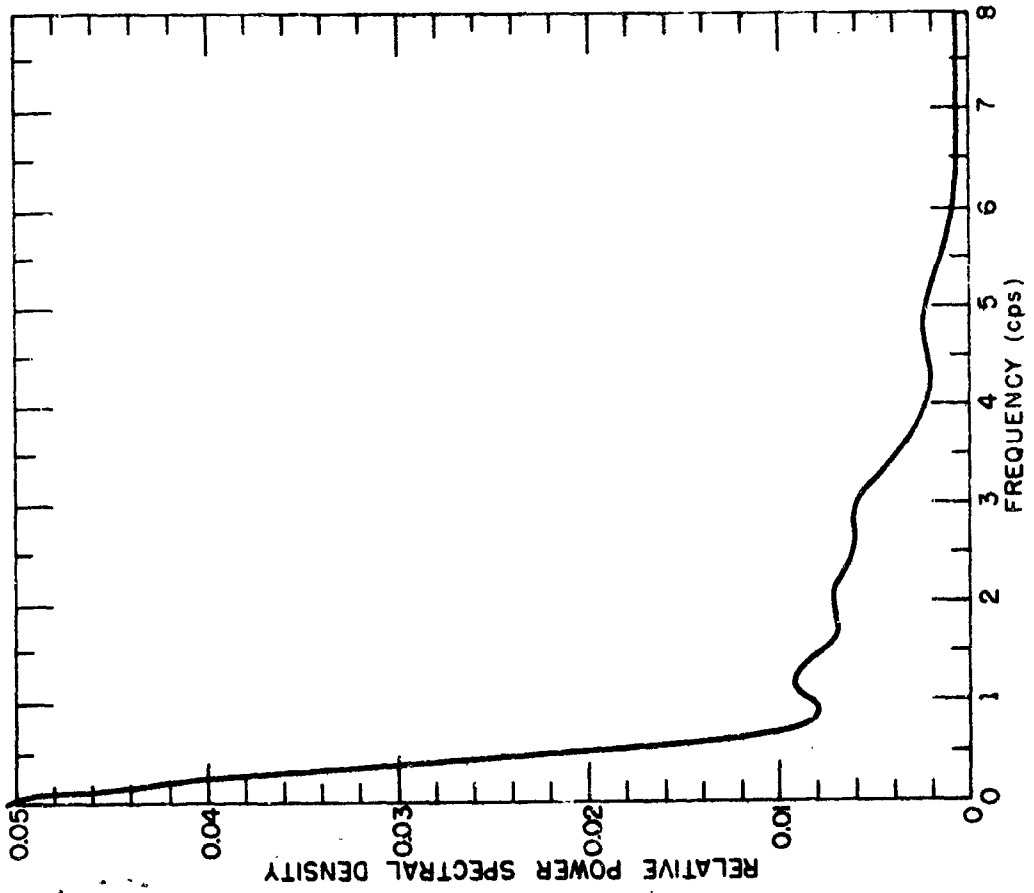

Fig. 10. Digital PSD curve of a cw signal reflected by Echo II during revolution 2626.

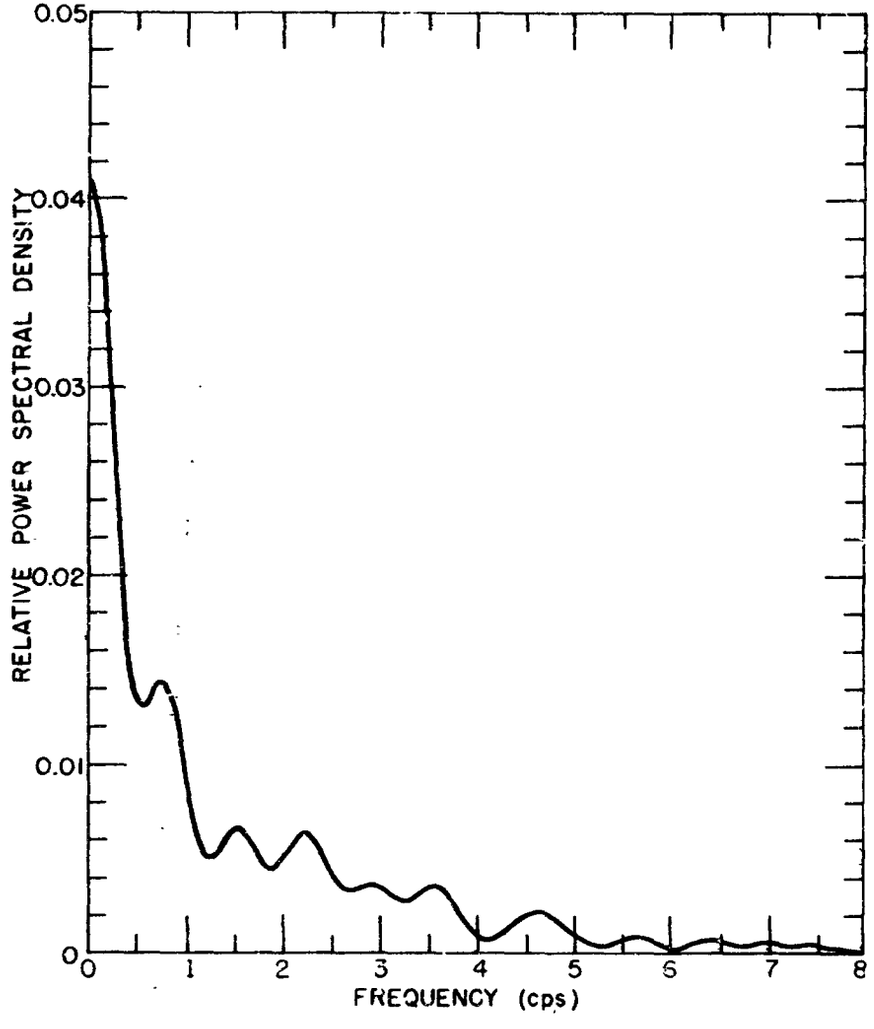

Fig. 12. Digital PSD curve of a cw signal reflected by Echo II during revolution 2816.

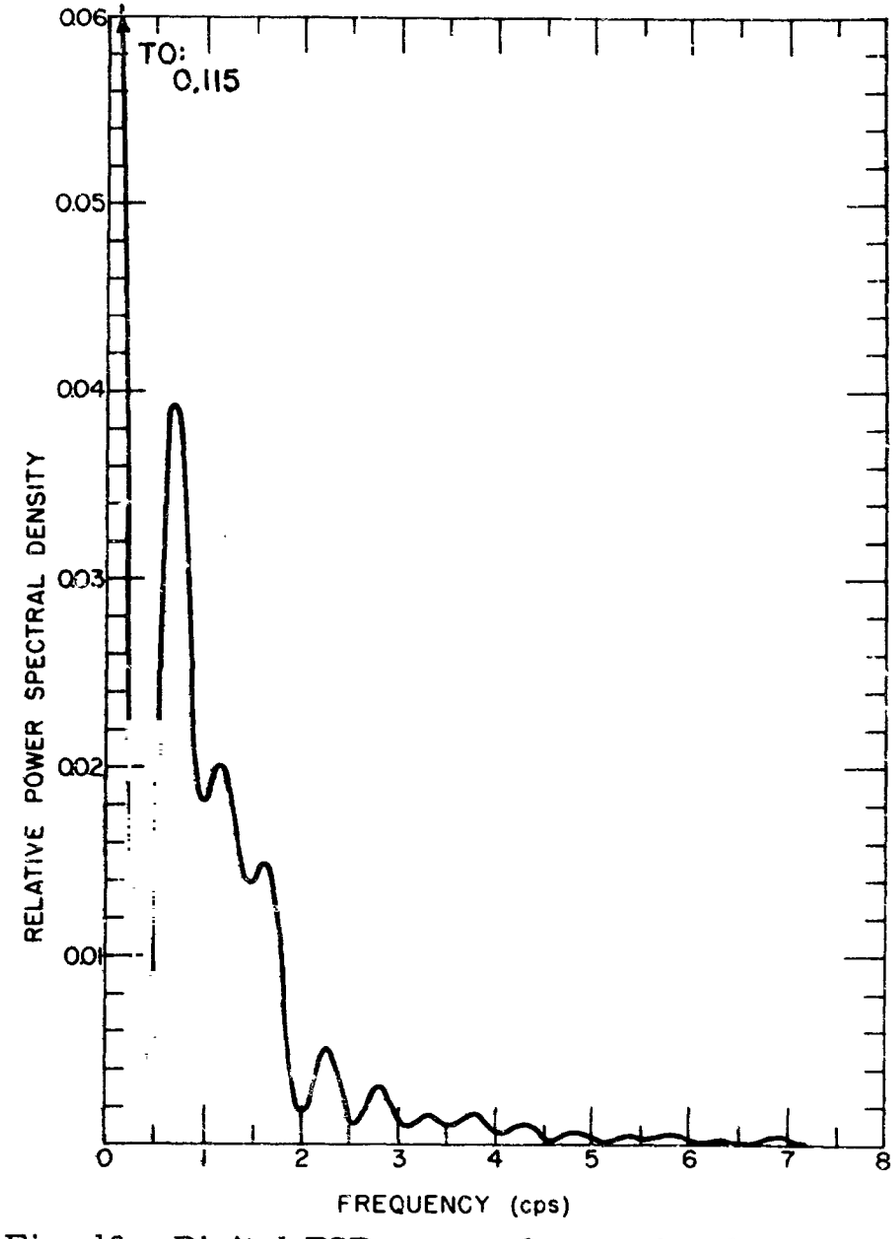

Fig. 13. Digital PSD curve of a cw signal reflected by Echo II during revolution 3040.

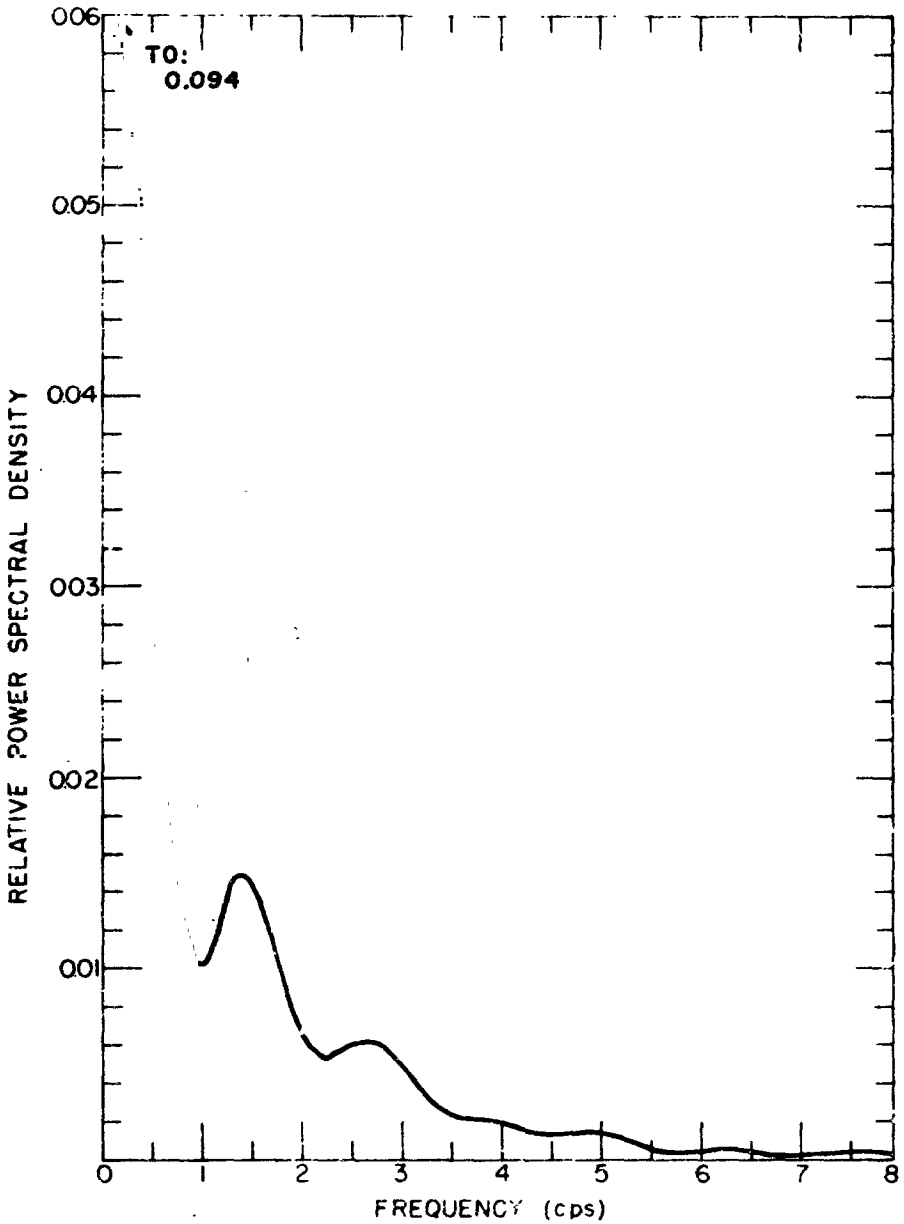

Fig. 14. Digital PSD curve of a cw signal reflected by Echo II during revolution 3483.

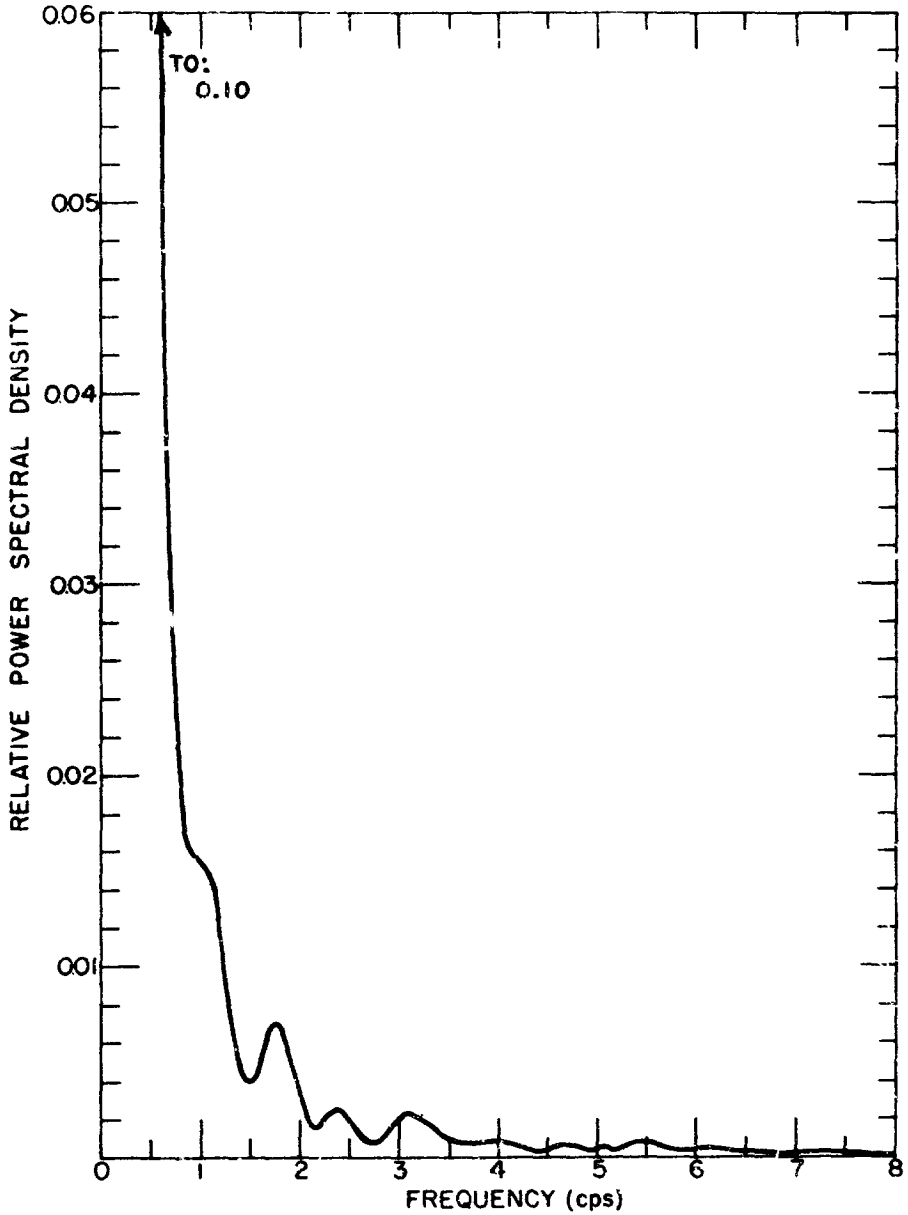

Fig. 15. Digital PSD curve of a cw signal reflected by Echo I during revolution 18,166.

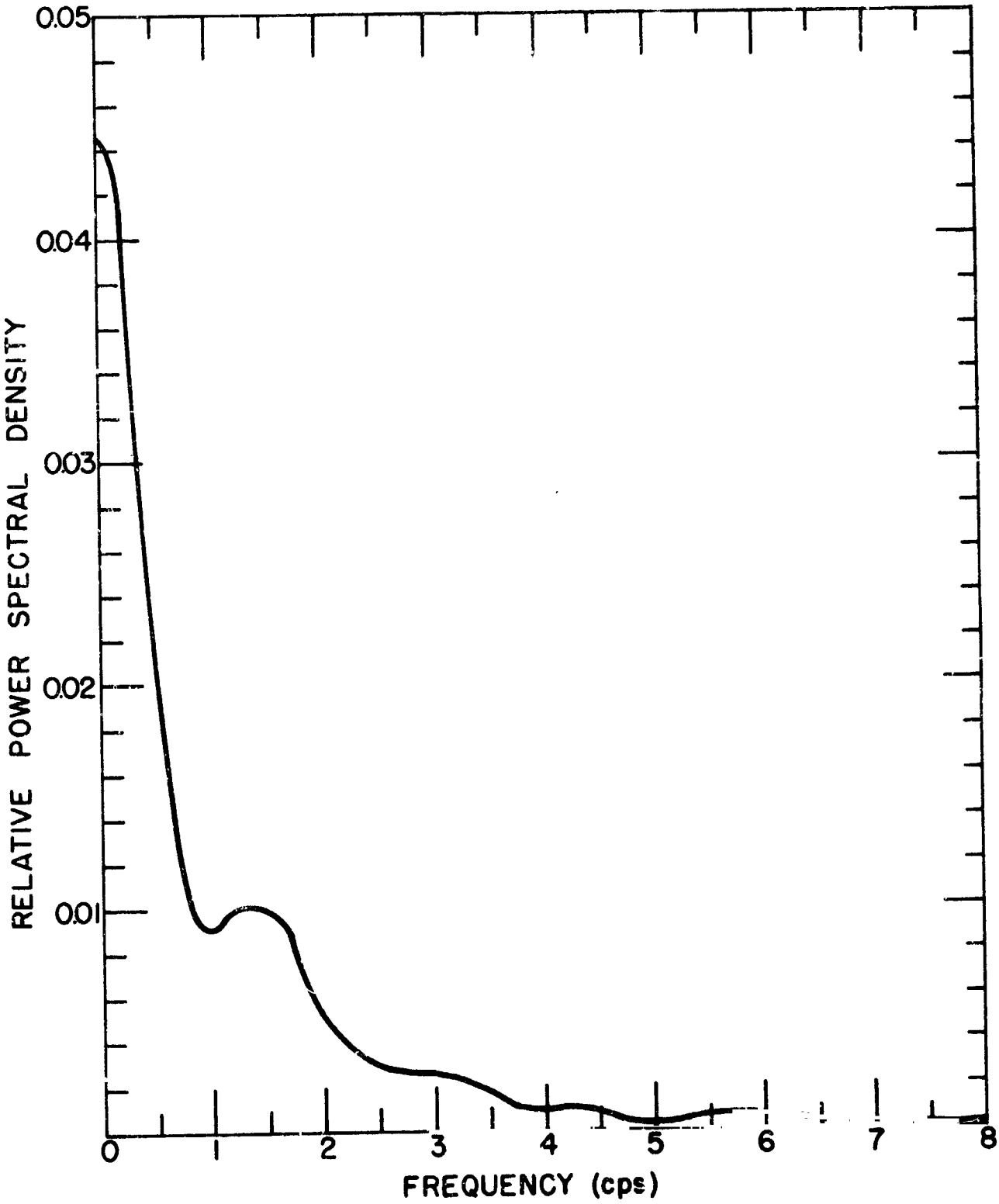

Fig. 16. Digital PSD curve of a cw signal reflected by Echo I during revolution 18,966.

V. ACKNOWLEDGEMENTS

The author is grateful to the personnel at the tracking site for the collection of the data: Messrs. D. Hayes, K. Reinhard, M. Gordon, and D. Landis, under the direction of R.C. Taylor; to Messrs. R. Christen, F. Cook, and R. Weber for their assistance in reducing the data; and to J. Reed for programming the computer.

Special thanks are due to Dr. R.T. Compton, Jr., for providing the PSD curves by the digital technique and for his valuable suggestions during the preparation of this report.

REFERENCES

1. Zolnay, S.L., "Power Spectral Density Analysis of Passive Satellite Reflected Signals," TDR II, Vol. 2, Antenna Laboratory, The Ohio State University Research Foundation; prepared under Contract AF 30(602)-2166 for Rome Air Development Center.

2. Compton, R.T., "The Surface Roughness of Echo II - A Preliminary Study," Report 1878-7, 31 December 1964, Antenna Laboratory, The Ohio State University Research Foundation; prepared under Grant NAS5-9507 for National Aeronautics and Space Administration.

3. Eberle, J.W., "An Adaptively Phased, Four-Element Array of Thirty-Foot Parabolic Reflectors for Passive (Echo) Communication Systems," TDR IV, Antenna Laboratory, The Ohio State University Research Foundation; prepared under Contract AF 30(602)-2166 for Rome Air Development Center.

4. Experiments Plan Passive Communications Satellite Echo II, M.H. Baker, 11 January 1964, Goddard Space Flight Center, National Aeronautics and Space Administration, Greenbelt, Maryland.

5. Groves, B.R., private communication.

6. Solodovnikov, V.V., Introduction to the Statistical Dynamics of Automatic Control Systems, p. 114, Dover Publications, Inc.,

7. Zolnay, S.L., "An Analysis of Echo II Reflected Signals at 2 KMC/sec," TDR II, Vol. 1, Antenna Laboratory, The Ohio State University Research Foundation; prepared under Contract AF 30(602)-2166 for Rome Air Development Center.

8. Eberle, J.W., "The Surface Roughness of Echo II, Echo I and the Moon as Obtained from Aplitude Fading Statistics," TDR II, Vol. 3, Antenna Laboratory, The Ohio State University Research Foundation; prepared under Contract AF 30(602)-2166 for Rome Air Development Center.

9. Eberle, J.W. and Zolnay, S.L., "Autocorrelation Functions of Echo II Reflected Signals," TDR III, Vol. 2, Antenna Laboratory, The Ohio State University Research Foundation; prepared under Contract AF 30(602)-2166 for Rome Air Development Center.

10. Zolnay, S.L. and Eberle, J.W., "The Long-term Autocorrelation Function of Echo II Reflected Signals," TDR III, Vol. 4, Antenna Laboratory, The Ohio State University Research Foundation; prepared under Contract AF 30(602)-2166 for Rome Air Development Center.

11. Suzuki, T., "Wave Forms and Ambiguity Functions of Pulsed Signals Reflected from a Spherical Satellite," Report 1878-1, 31 December 1964, Antenna Laboratory, The Ohio State University Research Foundation; prepared under Grant NAS5-9507 for National Aeronautics and Space Administration.

12. Suzuki, T., "Determination of a Pulse Train to Detect the Surface Characteristics of Echo II," Report 1878-2, 31 December 1964, Antenna Laboratory, The Ohio State University Research Foundation; prepared under Grant NAS5-9507 for National Aeronautics and Space Administration.

13. Zolnay, Stephen L., "Signal Strength Analysis of Echo II Reflected Signals at 2 KMC/sec (Revolutions 2000-3500)," Report 1878-3, 31 December 1964, Antenna Laboratory, The Ohio State University Research Foundation, prepared under Grant NAS5-9507 for National Aeronautics and Space Administration.

14. Zolnay, Stephen L., "Apparent Scattering Cross-Section of Echo II," Report 1878-4, 31 December 1964, Antenna Laboratory, The Ohio State University Research Foundation; prepared under Grant NAS5-9507 for National Aeronautics and Space Administration.

15. Zolnay, Stephen L., "Power Spectral Density of Echo II Reflected Signals," Report 1878-5, 31 December 1964, Antenna Laboratory, The Ohio State University Research Foundation; prepared under Grant NAS5-9507 for National Aeronautics and Space Administration.

16. Tourdot, James E., "Probability Density Function of the Envelope of a CW Signal Received over Echo II," Report 1878-6, 31 December 1964, Antenna Laboratory, The Ohio State University Research Foundation; prepared under Grant NAS5-9507 for National Aeronautic and Space Administration.

17. Compton, R.T., "The Surface Roughness of Echo II - A Preliminary Study," Report 1878-7, 31 December 1964, Antenna Laboratory, The Ohio State University Research Foundation; prepared under Grant NAS5-9507 for National Aeronautics and Space Administration.

18. Zolnay, Stephen L., "The Short Term (τ_{max} = 3 sec) Autocorrelation Function of Echo II Reflected Signals," Report 1878-8, Antenna Laboratory, The Ohio State University Research Foundation; prepared under Grant NAS5-9507 for National Aeronautics and Space Administration.

19. Zolnay, Stephen L., "The Long Term Autocorrelation Functions of Echo Reflected Signals," Report 1878-9, 31 December 1964, Antenna Laboratory, The Ohio State University Research Foundation; prepared under Grant NAS5-9507 for National Aeronautics and Space Administration.

20. Taylor, R.C., "A Comparison of the Surface Roughness of Echo I and II from the Direct and Cross Polarized Components at 2.26 KMC," Report 1878-10, 31 December 1964, Antenna Laboratory, The Ohio State University Research Foundation; prepared under Grant NAS5-9507 for National Aeronautics and Space Administration.

21. Hayes, D.D., "System Gain-to-Noise Temperature Ratio Measurements on an Adaptively-Phased Array," TDR I, Vol. 3, Antenna Laboratory, The Ohio State University Research Foundation; prepared under Contract AF 30(602)-2166 for Rome Air Development Center.

VI. APPENDIX

A. Data Collection, Reduction, and Analysis

This report is one of a series dealing with various aspects of Echo-reflected signals. There are actually two series of reports. The earlier series consisted of six reports on the following subjects: amplitude scintillations,[7] stationarity,[3] power spectral density,[1] probability density,[8] autocorrelation (short term),[9] and autocorrelation (long term).[10] The subjects considered in the present series are: determination of ambiguity function of signal,[11] signal requirements for determining surface of satellite,[12] amplitude scintillation,[13] apparent echo area,[14] power spectral density,[15] probability density,[16] scattering function,[17] autocorrelation (short term),[18] autocorrelation (long term)[19] and depolarization effects.[20] To ensure the successful completion of the planned series of reports some consideration must be given to data collection, reduction, and analysis. The purpose of this appendix is to cover the above three areas.

B. Data Collection

1. System Description

The receiving site is at The Ohio State University's Antenna Laboratory in Columbus, Ohio. The geodetic coordinates of the station are 083°02'30" West Longitude, 40°00'10" North Latitude. The receiving antenna is the tracking dish of the four-element, adaptively phased array. Aperture diameter is 30 feet, reflecting surface is of solid material, and surface accuracy in terms of $\lambda/16$ criterion is good to 15 Kmc/sec. The paraboloid is focal-fed; its gain is 42 $\pm$0.5 db over an isotropic antenna.[21] Polarization diversity is available: VP, HP, RCP, LCP. The method of tracking is amplitude monopulse. The antenna-mounte receiving components are shown in Fig. 17. The parametric amplifier in the sum channel has 20 db gain, noise figure between 2.3-3.0 db, and 3 db bandwidth of 30 Mc/sec. The noise figure of the mixer-preamplifier is 8.5 db on double sideband basis, the gain is 40 db, and the 3 db bandwidth is 8 Mc/sec. The first IF signal at 30 Mc/sec is brought down on coaxial cable to the equipment van.

The block diagram of the stabilized local oscillator is shown in Fig. The local oscillator is locked in frequency to a reference crystal the frequency of which is voltage controllable necessary for tracking the doppler shift, and it is locked in phase to another reference crystal. The local

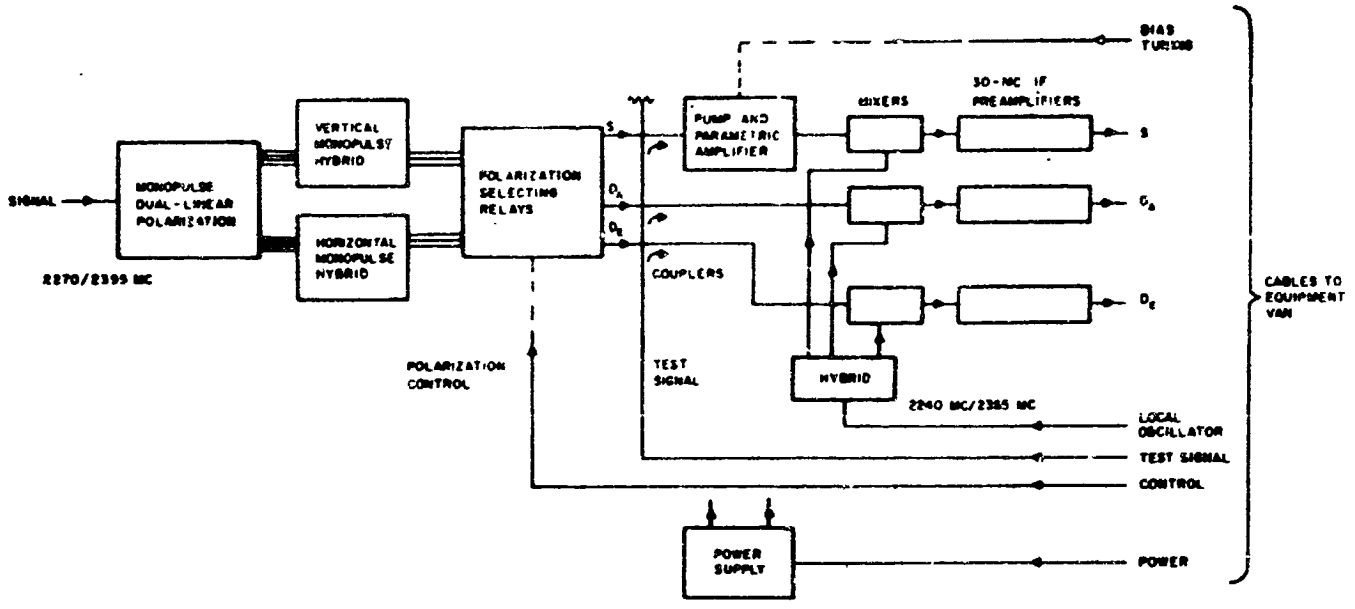

Fig. 17. Antenna-mounted receiving components.

oscillator can be made to track the frequency and/or phase of the incoming signal. The time constants in the loops of the oscillator can readily be adjusted for ease of acquisition or of tracking.

The IF signal-processing equipment is shown in Fig. 19. The gain of the 30 MC and 3 MC section of the receiver is typically 75 dbs, the useful range is about 20 dbs, and the bandwidth is successively narrowed to about 12 KC-s. The 2 MC outputs are down-converted to 455 Kc/sec and with the phase-lock demodulators are further down-converted to dc. Figure 20 gives the block diagram of the phase-locked demodulators. The output(s) of the phase-locked demodulators are recorded on magnetic tape and/or paper charts. Figure 21 shows a simplified block diagram of the system.

The specifications of the system are summarized below.

1. Location: (a) 083° 02' 30" West Longitude
   (b) 40° 00' 10" North Latitude
   (c) Center of radiation--830 feet above MSL

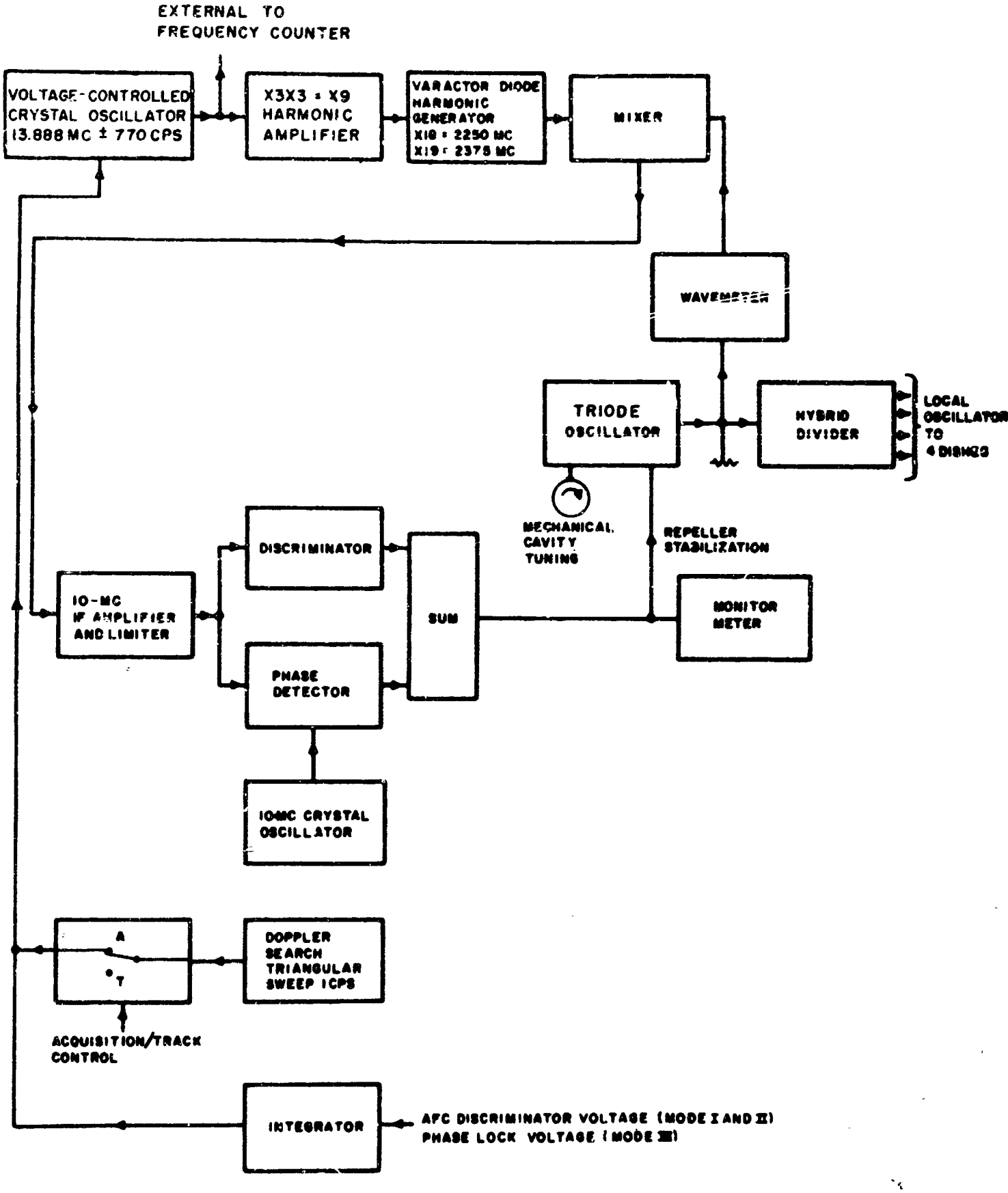

Fig. 18. Stabilized local oscillator.

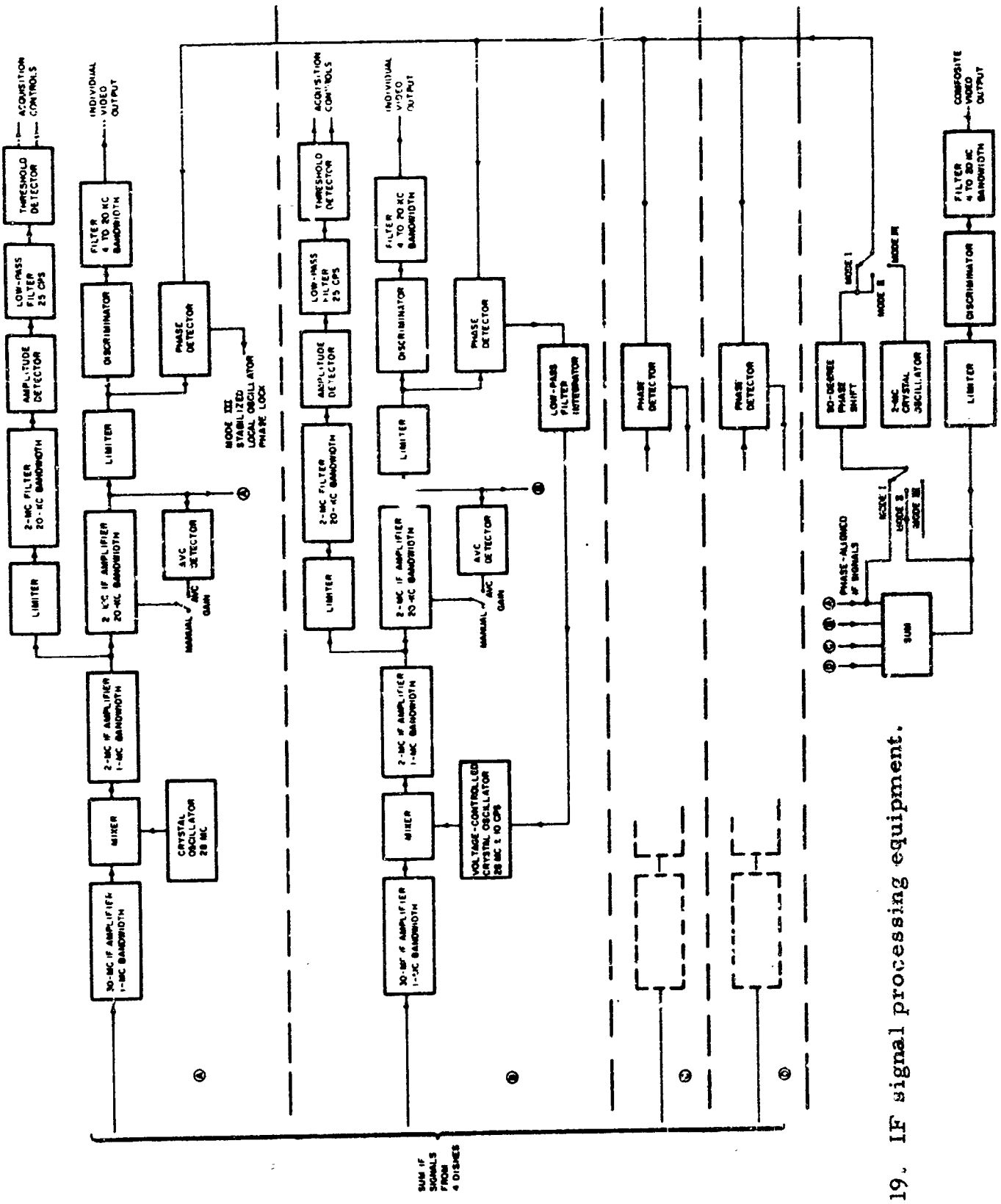

Fig. 19. IF signal processing equipment.

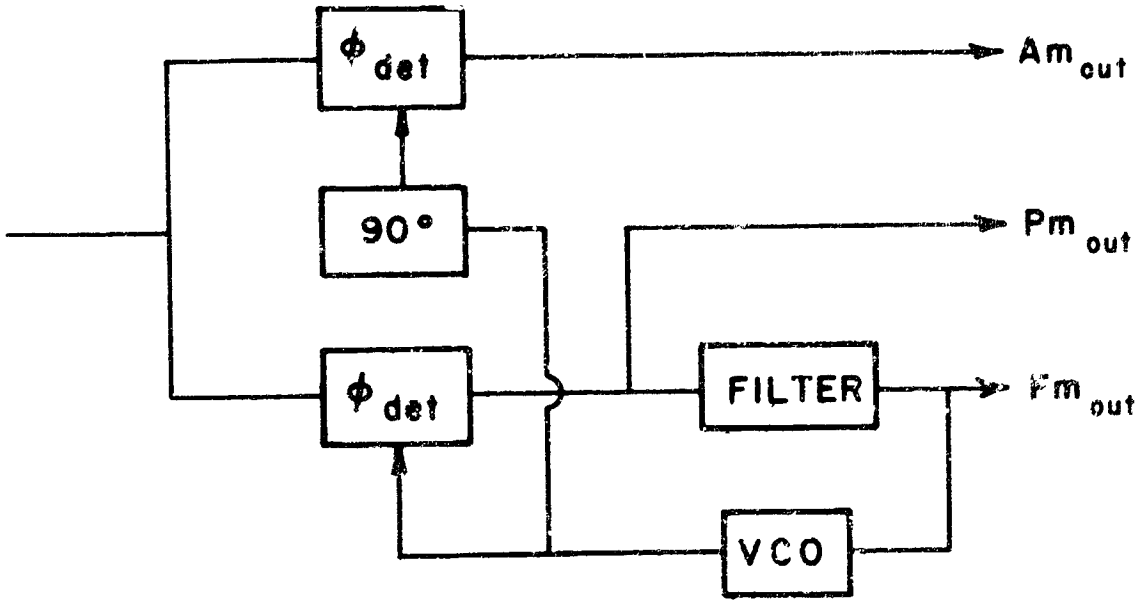

Fig. 20. Phase-locked demodulators.

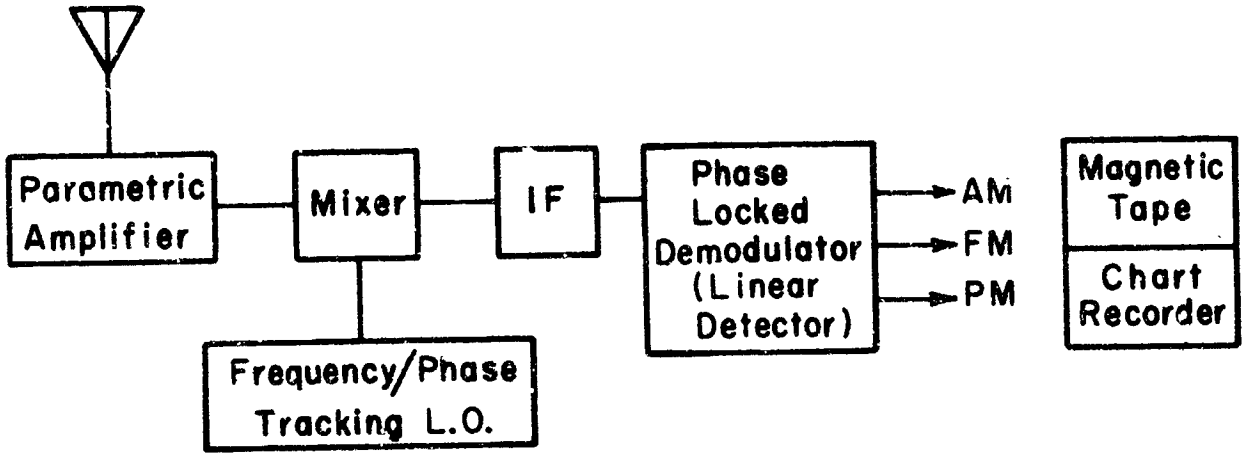

Fig. 21. Simplified block diagram of the system.

2. Antenna:
   (a) Type--paraboloid, solid surface, 0.040° RMS
   (b) Mounting--AZ/EL
   (c) Limits of movement--±360 in Azimuth
   -1° to 120° Elevation
   (d) Velocity limits--2°/sec Azimuth
   2°/sec Elevation
   (e) Acceleration limits--3°/sec^2 Azimuth
   3°/sec^2 Elevation
   (f) Pointing Accuracy--±0.01°
   (g) Beamwidth--1°
   (h) Polarization--Linear or Circular
   (i) Gain (measured)--42 ± 0.5 db at 2260 Mc

3. Phase-lock Tracking Receiver:
   (a) Frequency--2260 Mc
   (b) Tracking mode--phase or frequency lock
   (c) Noise figure--2.5 db
   (d) IF Frequency--30 Mc, 2.7 Mc, 455 Kc
   (e) Bandwidth-- 1 Mc/at 30 Mc, narrowed down to
   5 Kc at 455 Kc
   (f) Frequency tracking accuracy--10 cps at 10 Mc

4. Communication Receivers:
   (a) Frequency--30 Mc
   (b) IF frequency--2.7 Mc and 455 Kc
   (c) Bandwidths--12 Kc at 2.7 Mc, 5 Kc at 455 Kc
   (d) Outputs--AM, PM, FM

5. Tape Recorder, Magnetic:
   (a) Model--Ampex
   (b) Available channels--7, direct or fm
   (c) Tape Width--1/2 inch
   (d) Frequency response--0.1 to 12.5 Kc direct
   0 to 1.25 Kc fm

6. Tape Recorder, Paper:
   (a) Model(s)--1 Sanborn 150(2)
   1 Sanborn 350
   (b) Channels--4 + 8, total of 12
   (c) Speeds--1/4 to 100 mm/sec

2. Format for collected data

Prior to each time tracking of a target is attempted the established tuning and calibrating procedure is accomplished according to standard operational practices. The results of these procedures are recorded in the Station Log Book.

During tracking of Echo the following data will be recorded in the format given below:

Magnetic Tape Recorder:

Channel 1 AM output, South receiver, FM recording
Channel 2 AM output, North receiver, FM recording
Channel 3 AM output, East receiver, FM recording
Channel 4 AM output, West receiver, FM recording
Channel 5 Phase detector in master channel, FM recording
Channel 6 AM output, sum receiver, FM recording
Channel 7 Time and voice commentary, Direct recording

Paper Tape Recorder

I Channel 1 AM output, North receiver
Channel 2 AM output, East receiver
Channel 3 AM output, South receiver
Channel 4 AM output, West receiver

Tape Speed: 2 1/2 mm/sec

II Channel 1 AM output Sum Receiver
Channel 2 Relative Phase S-N baseline
Channel 3 Relative Phase S-E baseline
Channel 4 Relative Phase S-W baseline

Time will be indicated with ticks at every second; additionally one-minute markers will be provided and properly identified.

Digital Paper Tape:

VCO frequency directly proportional to doppler to the nearest cycle will be recorded as a function of local time to the nearest second. Immediately after the completion of the tracking the following form will be completed; additional comments noting any unusual circumstances or facilitating data reduction and analysis will also be noted.

1. TARGET
2. PASS NO.
3. DATE
4. ZEBRA TIME
5. EST. TIME HR MIN AM PM
6. TRANSMITTER FREQUENCY
7. POWER LEVEL
3. MODULATION
9. RECORDINGS

Power Level	South	North	East	West	Sum
27 MC Phase	S-N	S-W	S-E		
Monopulse Errors		Yes	No	Chart No.	
Position Indicators		Yes	No	Chart No.	
Slave Errors	North	East	West		
Discriminator		Yes	No		
2.7 MC Phase Detectors		South	North	East	West
455 KC Phase Detectors		South	North	East	West
Doppler		Yes	No	Chart No.	

10. TAPE RECORDER Tape Number

Channel	1	Direct	FM
	2	Direct	FM
	3	Direct	FM
	4	Direct	FM
	5	Direct	FM
	6	Direct	FM
	7	Direct	FM

11. 4 CHANNEL SANBORN CHART NUMBER

Channel	1	Calibration	Yes	No
	2	Calibration	Yes	No
	3	Calibration	Yes	No
	4	Calibration	Yes	No

12. 8 CHANNEL SANBORN CHART NUMBER

Channel	1	Calibration	Yes	No
	2	Calibration	Yes	No
	3	Calibration	Yes	No
	4	Calibration	Yes	No
	5	Calibration	Yes	No
	6	Calibration	Yes	No
	7	Calibration	Yes	No
	8	Calibration	Yes	No

13. RECEIVER BANDWIDTHS (3 db)

North	KC	East	KC	West	KC
South	KC				

14. POLARIZATION OF ANTENNAS

North	VP	HP
East	VP	HP
West	VP	HP
South	VP	HP

15. TRANSMITTED POLARIZATION VP HP

16. NOISE FIGURE OF PARAMPS

North DB, East DB, West DB, South DB

17. BANDWIDTHS OF PARAMPS (3 db points)

North	KMC	to	KMC
East	KMC	to	KMC
West	KMC	to	KMC
South	KMC	to	KMC

18. LOCAL OSCILLATOR LOOP AFC Phase Lock

19. GAIN OF RECEIVERS

North DB, East DB, West DB, South DB

20. PHOTO OF POSITION DIALS Yes No

21. PHOTO OF TARGET Yes No

22. INTERVALS OF (20) sec, (21) sec.

23. COMMENTS

Data Rating

Crew Members

Other

C. Data Reduction and Analysis

1. Signal strength

Paper tape charts giving the AM output of the master tracking antenna will be utilized. This recording is directly proportional to the instantaneous received power level or signal strength. The measured power level can be expressed as relative to the noise level of the system with no signal input. The calculated power level is based on the radar range equation. The comparison between these levels is made by expressing the levels in terms of the signal-to-noise ratio, S/N. The noise figure, NF, of a receiver is given by the relationship

$$(1) \qquad NF = \frac{N_R + N_i}{N_i} \quad ,$$

where N_R and N_i are the noise components due to the receiver and the input noise, respectively. The input noise, N_i, is the product of the ambient temperature, Boltzman's constant, and the bandwidth:

$$(2) \qquad N_i = T_{ambient} \times 1.38 \times 10^{-23} \frac{\text{joules}}{^\circ K} \times \Delta f.$$

Hence,

$$(3) \qquad N_r = (NF-1)N_i = (NF-1)(270) \times 1.38 \times 10^{-23} \times \Delta f \text{ watts.}$$

One must consider, however, additional contributions from the antenna temperature. For convenience one can lump into the term "antenna temperature" the not quite absolute zero sky toward which the main lobe of the antenna is directed (measurements of antenna temperature were carried out with the antenna pointing to Zenith); the back-lobe pickup from the Earth at ambient temperature; possible celestial sources in the far side lobes; and losses in the transmission lines, switches, and connectors. The average value of the antenna temperature is 100°K.[31] Thus the noise power output at the receiver output is

$$(4) \qquad P_N = N_R + N_A \text{ watts;}$$

(5) $$P_N = (NF-1)N_i+N_A = [(NF-1)\ 270 + 100]\ 1.38 \times 10^{-23} \times \Delta f \text{ watts.}$$

The noise figure is 2.5 db and the narrowest bandwidth in the system is 12 kc. Substituting these values into Eq. (4), one obtains

(6) $$P_N = [(1.78-1)\ 270+100] \times 1.38 \times 10^{-23} \times 1.2 \times 10^{-4} \text{ watts;}$$

$$P_N = 10 \log_{10}[3.73 \times 1.38 \times 10^{-17}] = -163 \text{ dbw.}$$

The result given in Eq. (6) was used as the calibration level relative to which the measured power level was expressed as so many db above the noise level of -163 db.

Having established that the noise level is the -163 dbw level, utilize the calibration curve provided prior to and after the tracking to establish a scale in steps of one db against which the instantaneous power level can be determined.

To obtain an absolute measurement one can consider the method of calibration itself which was carried out by inserting a 30 Mc/sec signal of known amplitude (-99 dbw) and adjusting the receiver and demodulator gains to yield one volt dc output (full scale deflection). By combining this figure with the measured gains of the parametric amplifiers and of the 30 Mc preamplifiers, and with the measured line losses, one can readily arrive at a measured figure for a given power level necessary to give full deflection.

After having established two levels by two different methods the calibration curve provided prior to the pass is utilized to obtain a value for the instantaneous received power level. From the instaneous recording there will also be made an averaged recording. The average received power level (time constant, $\tau \approx 0.1$ second) will also be evaluated against the calibration scale on which the two levels described above have been established. High-speed recordings, when needed, will also be made. The data will be analyzed primarily for establishing the existence and severity of amplitude scintillations. This will be done by comparing the measured signal strength with the calculated one.

The following is an IBM 1620 computer program using OSU's version of Fortran to solve the radar range equation. The parameters, with the exception of P_T, d_R, and d_T, were lumped into a single constant, K. The value for K is given below for ranges in kilometers.

```
   80 READ 3,IND1,N1,N2,N3,N4,N5,PT,FK
    3 FORMAT (I1,I7,I5,I3,I5,I7,F7.3,E15.8)
   65 GO TO (20,30,40,80),IND1
   20 PUNCH 2
      PUNCH1
    1 FORMAT (9H  PASS NO5X4HDATE6X5HZDATE)
      PUNCH 2,N1,N2,N3,N4,N5,PT,FK
    2 FORMAT (I8,I5,I3,I5,I8,5H  PT=,F6.3,4H  K=,E14.8)
      PUNCH 2
      PUNCH 4
    4 FORMAT (8H   ZTIME4X2HDR5X2HDT10X2HPR9X9H10LOG10PR)
      PUNCH 2
      K= FK*1.E+02
      IF (K) 50,55,50
   50 PUNCH 5
      GO TO 60
   55 PUNCH 6
    5 FORMAT (4X21HHRMN RANGE,KILOMETERS5X5HWATTS10X3HDBW)
    6 FORMAT (4X20HHRMN  RANGE,NAUT,MI,6X5HWATTS10X3HDBW)
   60 PUNCH 2
   70 READ 7,IND1,JTIME,JDR,JDT
    7 FORMAT (I1,I7,I7,I7)
      GO TO 65
   30 DR= JDR
      DT= JDT
      PR= PT*FK/(DR*DR*DT*DT)
      FLOG= 4.3429448*LOG(PR)
      PUNCH 8,JTIME,JDR,JDT,PR,FLOG
    8 FORMAT (I8,I7,I7,E17.8,F10.1)
      GO TO 70
   40 PUNCH 2
      PUNCH 9
    9 FORMAT (6X3HEND)
      PUNCH 2
      STOP 9999
      END
```

$$K_{km} = 0.44581132 \times 10^{-1}.$$

The inputs to the program are transmitted power P_T, in myriawatts; ranges d_R, d_T as functions of time; the correct value of K; and identifying information, i.e., pass number, date, and Zebra date.

2. Echo area

The instantaneous signal strength recording from the magnetic tape will be re-recorded on paper tape after passing the data through an integrator whose time constant is two seconds. The computed level will be plotted on the chart, which corresponds to the theoretical cross section of the satellite for all bistatic angles between The Ohio State University and Dallas. Where applicable, i.e., where the data are not interrupted nor saturated, the pen deflection will be measured every two seconds relative to the calculated level and expressed in terms of decibels with the aid of the calibration curve. The data will be analyzed to yield primarily measured scattering cross section of Echo II, and plotted to show these two-second averaged measurements as so many decibels relative to the calculated scattering cross section.

3. Autocorrelation, probability density, and power spectral density functions

To obtain the above functions the data will be reduced by two methods: digital and analog. Each method will be described.

a. Digital method

To reduce the data by the digital method high-speed oscillographic recordings will be made from the magnetic tape of the instantaneous signal level (AM output of the demodulator). This recording will be sampled at least 50 times per second with an amplitude resolution of ± 1 count ranging from zero(noise level) to 100 (saturation level). Punched cards compatible with the computer program given below will be prepared from these sampled data. The calibration curve obtained from the start of the magnetic tape will be accurately plotted and approximated in the computer by a tenth-order polynomial; thus an accurate correction factor will be obtained for each sampled data point. This correction factor will be such that the data will be linearized. The purpose of the computer program is to yield the autocorrelation, probability density, and power spectral density functions of Echo-reflected signals. The output of the computer will be plotted and analyzed. This program is given below.

SOURCE LANGUAGE STATEMENTS

```
 1 C              CALCULATION OF PDF, ACF, AND PSD USING LINEARIZED INPUT DATA.-
 2                DIMENSION (A(196,NA),C(20),F(IA),P(103),PHI(18),X(20),Y(20))-
 3   START        READ INPUT ,FMT2,(JCT,X(1),X(2),X(3),X(4),X(5),X(6),X(7),X(8),X(9),X(10),ND)-
 4                TRANSFER (STOP) PROVIDED (JCT.E.2)-
 5                PI2=6.2831853-
 6                NA=14-
 7                WRITE OUTPUT ,FMTJ-
 8                NN=ND+1-
 9                READ INPUT ,FMT3,(A(1,NN),A(2,NN),A(3,NN),A(4,NN),A(5,NN),A(6,NN) A(7,NN),A(8,NN),A(9,NN),A(10,NN))-
10                DO THROUGH (A10),I=1,1,I.LE.ND-
11                DO THROUGH (A10),J=1,1,J.LE.ND-
12   A10          A(I,J)=X(I).P.J-
13                DO THROUGH (A18),LI=1,1,LI.LE.ND-
14                LLL=LI-1-
15                DO THROUGH (A18),I=LI,1,I.LE.ND-
                  II=I+1-
17                DO THROUGH (A17),K=1,1,K.LE.LLL-
18                A(I,LI)=A(I,LI)-A(I,K)*A(K,LI)-
19   A17          A(LI,II)=A(LI,II)-A(LI,K)*A(K,II)-
20   A4           A(LI,II)=A(LI,II)/A(LI,LI)-
21   A18          CONTINUE -
22                DO THROUGH (A23),LI=2,1,LI.LE.ND-
23                I=NN-LI-
24                II=I+1-
25                DO THROUGH (A22),K=II,1,K.LE.ND-
26   A22          A(I,NN)=A(I,NN)-A(I,K)*A(K,NN)-
27   A23          CONTINUE -
28                DO THROUGH (A30),I=1,1,I.LE.ND-
```

```
                C(I)=A(I,NN)-
                INDEX=0-
CASEA           INDEX=INDEX 1-
                 READ INPUT ,FMT6,(JCT,X(1),X(2),X(3),X(4),X(5),X(6),X(7),X(8),X(9),X(10),X(11),X(12),X(13),X(14),X(1
                     5),X(16),X(17),X(18))-
                 TRANSFER (SECB) PROVIDED (JCT.G.0)-
                 WRITE OUTPUT ,FMT8,(X(1),X(2),X(3),X(4),X(5),X(6),X(7),X(8),X(9),X(10),X(11),X(12),X(13),X(14),X(15)
                     ,X(16),X(17),X(18),INDEX)-
                 DO THROUGH (A45),I=1,1,I.LE.18-
                ISUM=18*(INDEX-1)+I-
                F(ISUM)=C(1)*X(I)-
                Z=X(1)-
                 DO THROUGH (A40),J=2,1,J.LE.ND-
                Z=Z*X(I)-
A40             F(ISUM)=F(ISUM)+C(J)*Z-
A45             Y(I)=F(ISUM)-
A50              WRITE OUTPUT ,FMT7,(Y(1),Y(2),Y(3),Y(4),Y(5),Y(6),Y(7),Y(8),Y(9),Y(10),Y(11),Y(12),Y(13),Y(14),Y(15)
                     ,Y(16),Y(17),Y(18),INDEX)-
                 TRANSFER (CASEA)-
F FMT2          (I1,F5.1,9F4.1,I18)      -
F FMT3          (10F4.1)     -
F FMT6           (I1,F3.1,17F4.1)-
F FMT7          (4H OUT,F7.1,17F6.1,I6) -
F FMT8           (3HOIN,F8.1,17F6.1,I6) -
SECB             I7=X(7)/10.-
                 I8=X(8)/10.-
                 I9=X(9)/10.-
                 REAL=10.*X(1)+.01*I7-
                 REAU=10.*X(2)+X(7)/10.-I7-
                 RAAL=10.*X(3)+.01*I8-
                 RAAU=10.*X(4)+X(8)/10.-I8-
```

```
57              RSNL=10.*X(5)+.01*I9-
58              RSNU=10.*X(6)+X(9)/10.-I9-
59              INC=X(11)-
60              AIDT=X(12)-
61              AIX=X(13)-
62              IRUN1=X(14)-
63              IRUN2=X(15)*10.-
64              RUN3=X(16)-
65              RUN4=X(17)-
66              IRUN5=X(18)*10.+.01-
67              NIX=18*INDEX-
68              INTEGR=AIX*AIDT/(INC*2)-
69              IX=INTEGR*2*INC-
70              N=NIX-IX-
71              T=N/AIDT-
72               TRANSFER TO (CASED) PROVIDED (JCT.E.4.OR.JCT.E.5)-
73               WRITE OUTPUT ,FMTB,(IRUN1,IRUN2,RUN3,RUN4,IRUN5,REAL,REAU,RAAL,RAAU,RSNL,RSNU,AIDT,T,N,IX)-
74              P(0)=0.-
75               DO THROUGH (CASER),I=1,1,I.LE.101-
76              P(I)=0.-
77               DO THROUGH (CASEY),L=1,1,L.LE.NIX-
78               TRANSFER TO (CASEY) PROVIDED (F(L).L.(I-1).OR.F(L).GE.I)-
79              P(I)=P(I)+1.-
80  CASEY        CONTINUE -
81  CASER        WRITE OUTPUT ,FMTF,(I,P(I)/NIX)-
82               TRANSFER TO (START) PROVIDED (JCT.E.3)-
83  CASED        WRITE OUTPUT ,FMTH,(IRUN1,IRUN2,RUN3,RUN4,IRUN5,REAL,REAU,RAAL,RAAU,RSNL,RSNU,AIDT,T,N,IX)-
84               DO THROUGH (CASEB),I=0,INC,I.LE.IX-
85  PQD         PHI(I)=0.-
```

```
      DO THROUGH (CASEC),K=1,1,K.LE.N-
CASEC PHI(I)=PHI(I)+F(K)*F(K+I)-
      TRANSFER TO (CASEE) PROVIDED (I.G.0)-
      PHIA=PHI(0)-
CASEE PHI(I)=PHI(I)/PHIA-
CASEB  WRITE OUTPUT ,FMTD,(I,PHI(I))-
      TRANSFER TO (START) PROVIDED (JCT.E.4.OR.JCT.E.6)-
F FMTB (1H14X68HPROBABILITY DENSITY FUNCTION FOR PAS  VE SATELLITE REFLECTED SIGNALS
                              /10X4HRN =,I3,I4,F5.   5.1,I4 // 5X20HRANGE OF ELEVATION = F6.2,1H, ..2,4HDEG
     .5X18HRANGE OF AZIMUTH =F7.2,1H,F8.2,4HDEG.//5X18HRANGE OF (S+N)/N =F8.2,1H,F9.2,3HDB.//5X11HDEL
     TA T =1/F4.0,5X3HT =F6.2,5X3HN =I5,5X3HX =I5//) -
F FMTC (18F4.1)    -
F FMTD   (10X4HPHI(I4,3H) =F10.6)    -
F FMTE (18F6.1)    -
F FMTF (12X2HP(I4,3H) =F10.6)  -
F FMTG (10X2HS(I4,3H) =,F10.6) -
F FMTH (1H14X65HAUTO CORRELATION FUNCTION FOR PASSIVE SATELLITE REFLECTED SIGNALS
                              /10X4HRN =,I3,I4,F5.1,F5.1,I4 // 5X20HRANGE OF ELEVATION = F6.2,1H,F7.2,4HDEG
     .5X18HRANGE OF AZIMUTH =F7.2,1H,F8.2,4HDEG.//5X18HRANGE OF (S+N)/N =F8.2,1H,F9.2,3HDB.//5X11HDEL
     TA T =1/F4.0,5X3HT =F6.2,5X3HN =I5,5X3HX =I5//) -
F FMTI (1H14X71HPOWER SPECTRAL DENSITY FUNCTION FOR PASSIVE SATELLITE REFLECTED SIGNALS
                              /10X4HRN =,I3,I4,F5.1,F5.1,I4 // 5X20HRANGE OF ELEVATION = F6.2,1H,F7.2,4HDEG
     .5X18HRANGE OF AZIMUTH =F7.2,1H,F8.2,4HDEG.//5X18HRANGE OF (S+N)/N =F8.2,1H,F9.2,3HDB.//5X11HDEL
     TA T =1/F4.0,5X3HT =F6.2,5X3HN =I5,5X3HX =I5//) -
F FMTJ (1H118X73HINPUT DATA FOR FOLLOWING OUTPUT (IDENTIFY OUTPUT BY 6 DIGIT NUMBER ABOVE))-
STOP   CALL SUBROUTINE ()=ENDJOB.()-
       END PROGRAM (START)-
```

An additional computer program is available to compute the PSD from the ACF. This will be done as follows:

The ACF produced with the aid of the preceding program will be plotted. This graph will, in turn, be approximated with straight-line segments (as many as necessary to obtain accurate fit to the original curve), and the τ and $\phi(\tau)$ values at the break points tabulated. Further, the mean square average value of the ACF will be ascertained. It is estimated that this can be done within 15% for the ACFs produced. The τ and $\phi(\tau)$ values mentioned above and the estimated mean square average value will serve as inputs to the program given below. The output of this program will be a PSD curve which is estimated to have a frequency resolution of 1/3 of a cycle and an upper limit of 13 cps. These PSD curves will be analyzed for the frequency content of the unwanted amplitude modulation (fading) on the cw signal.

b. Analog method

The block diagram shown in Fig. 22 illustrates the analog manner by which the power spectral density curves of a signal are obtained. The

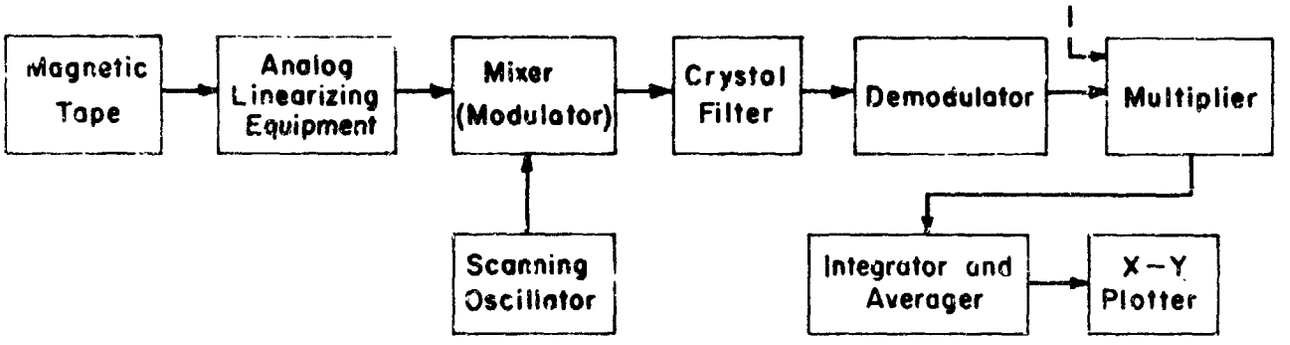

Fig. 22. Analog power spectral density analyzer.

output of the detector is simultaneously recorded on chart paper for visual display and on magnetic tape for data processing. The data on the magnetic tape are re-recorded on a 30-second tape loop. This loop is repeatedly played into a wave analyzer wherein it is used to modulate a 97 Kc/sec carrier. This relatively high frequency permits

COMPTON, R. T., JR. DEC 1, 1964

COMPUTED F3D FROM ACF BY FOURIER TRANSFORM
SOURCE LANGUAGE STATEMENT

```
F  F1          (I8) -
F  F2          (2F16.4)-
F  F3          (1P2E16.4)-
               DIMENSION (S(200), F(200), SL(200)) -
 START         READ INPUT, F1, (NO)-
               DO THROUGH (L5), M=1, 1, M. LE. NO-
               READ INPUT, F1, (N)-
               READ INPUT, F2, (F(1), S(1)) -
               DO THROUGH (L1), I=2, 1, I. LE. N-
               READ INPUT, F2, (F(I), S(I))
 L1            SL(I) = (S(I)-S(I-1))/(F(I)-F(I-1)) -
               TRO = 0. -
               DO THROUGH (L4) , KI=3, 1, KI. LE. N-
 L4            TRO=TRO + (SL(KI)-SL(KI-1))*(F(KI-1). P. 2)/2. -
               TRO= TRO-SL(N)*(F(N). P. 2)/2. -
               X= 0. -
               TX=1. 0-
               WRITE OUTPUT, F3,(X, TX) -
               READ INPUT, F2, (DELTA) -
               READ INPUT, F1,(J)-
               ETA=DELTA-
               DO THROUGH (L2), L=1, 1, L. LE. J-
               TR=SL(2) -
               DO THROUGH (L3), K=3, 1, K. LE. N-
 L3            TR=TR+(SL(K)-SL(K-1))*COS. (F(K-1)*ETA) -
               TR=TR-SL(N)*COS. (F(N)*ETA) -
               TR=-TR/(TRO*(ETA. P. 2))-
               WRITE OUTPUT, F3,(ETA, TR) -
 L2            ETA=ETA+DELTA-
 L5            CONTINUE-
               END PROGRAM (START)-
```

the use of crystal filters of selectable bandwidths of 2, 10, or 50 cps. After demodulation, the energy contained in the selected bandwidth reaches the multiplier stage, after which the averaging and integrating process is completed and the output is recorded on an x-y plotter as a function of frequency. The frequency of the oscillator producing the carrier is caused to scan at the same rate as the tape-loop is being repeated, i.e., if a crystal filter of 2 cps bandwidth is selected and the sample length is 50 seconds, the carrier frequency is shifted 2 cps during the same time. The amplitude of the resultant curve is proportional to the energy in the bandwidth selected by the crystal filter, centered on the frequency determined by the scanning oscillator from whose frequency, in turn, the frequencies present in the data can be determined. Simply, the entire operation is equivalent to finding the energy in the signal in a given bandwidth as this bandwidth is scanned from dc through audio frequencies, i.e., it is equivalent to finding the power spectral density of the signal.

Analog equipment is also available to produce autocorrelation and probability density functions of Echo-reflected signals, however these will not be described here since it is anticipated that improved results will be obtained from the digitized data.

4. Depolarization effects

To determine depolarization effects data will be collected on signal strength, with one antenna polarized the same as the transmitted signal and another antenna oppositely polarized. The data will be reduced in a manner similar to that described in Sections A and B above and will be analyzed to determine the magnitude of the cross polarized component relative to the direct received component of the signal. The above data reduction and analysis are suitable for most of the subjects to be covered in the present series of planned reports. The subjects of some of these reports are purely theoretical and at least one report is based on data already obtained. Hence, no data reduction and analysis plan will be included for these reports.